Journal of Medicinal Chemistry

pubs.acs.org/jmc

Article

Structure–Activity Relationship Study of Amidobenzimidazole Analogues Leading to Potent and Systemically Administrable Stimulator of Interferon Gene (STING) Agonists

Zilan Song,[#] Xiyuan Wang,[#] Yan Zhang,[#] Wangting Gu, Ancheng Shen, Chunyong Ding, Han Li, Ruoxuan Xiao, Meiyu Geng, Zuoquan Xie,* and Ao Zhang*

Cite This: *J. Med. Chem.* 2021, 64, 1649–1669

Read Online

ACCESS | Metrics & More | Article Recommendations | Supporting Information

ABSTRACT: Activation of the stimulator of interferon gene (STING) has emerged as an exciting immuno-oncology therapeutic strategy; however, the first-generation STING agonists, cyclic dinucleotide (CDN) analogues, have suffered from many disadvantages and failed in clinical trials. Therefore, non-CDN small-molecule STING agonists are urgently needed. In view of the unique structure of the high potency of dimeric amidobenzimidazole STING agonist **5**, a structural elaboration was conducted by modifying several structural hotspots of this scaffold. Triazole **40** was identified as a new potent STING activator, possessing EC_{50} values of 0.24 and 39.51 μM for h- and m-STING, respectively. This compound has a slightly better pharmacokinetic profile and is >20-fold more aqueously soluble than **5**. It activated the STING signaling dramatically by directly binding and stabilizing all h-STING isoforms and m-STING. In vivo, intermittent administration of **40** was found to have significant antitumor efficacy with good tolerance in two mouse tumor models.

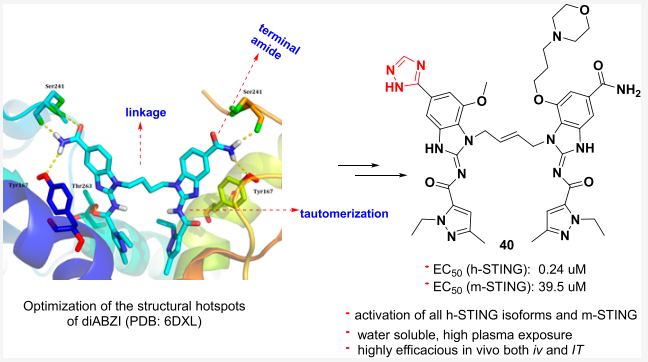

INTRODUCTION

The human immune system including innate and adaptive immunity is precisely controlled by a number of costimulatory and coinhibitory signaling molecules.[1] Aberrations of these immune signaling pathways can cause many diseases including cancer. In the past decade, the successful launch of several monoclonal antibodies (mAbs) targeting the suppressive immune checkpoint proteins has established a new era of immuno-oncology (IO) therapy as a vibrant cancer treatment.[2,3] However, compared to the success of checkpoint inhibitors, development of small molecules targeting the immunostimulatory signaling proteins is still in the infancy with much unknown and challenge.[4−6] The stimulator of interferon gene (STING) is a stimulatory molecule residing on the endoplasmic reticulum and plays a pivotal role in innate immunity by acting as a downstream sensor of both exogenous and endogenous DNA.[7−9] 2′,3′-cGAMP (Figure 1), a cyclic dinucleotide (cyclic GMP-AMP) synthesized by cyclic guanosine monophosphate (GMP)-adenosine monophosphate (AMP) synthase (cGAS) upon detecting tumorous or virus DNA in the cytosol, has been found as the endogenous ligand of STING.[10] Binding of STING with 2′,3′-cGAMP activates STING by forming dimers or oligomers resulting in downstream signaling cascade via recruitment of the serine/threonine protein kinase (TBK1), phosphorylation of the interferon regulatory transcription factor IRF3, and production of type I interferon (IFN) as well as many other proinflammatory cytokines.[11−13] These events can eventually result in promotion of the adaptive immune response by activation of cytotoxic CD8 T cells. Therefore, pharmacological activation of STING by agonists has emerged as an exciting yet challenging strategy of IO therapy for various diseases such as cancer, virus, and autoimmune diseases.[14−16]

Many efforts have been focused on STING agonists by developing chemically more stable cyclic dinucleotide (CDN) analogues of 2′,3′-cGAMP, resulting in the most upfront compound **1** (ADU-S100, Figure 1) bearing dithio-mixed linkages.[17] This compound significantly enhanced STING signaling by inducing much higher levels of IFN-β and showed remarkably tumor growth suppression or even regression in several mice models, including BALB/c mice bearing CT26 colon and 4T1 mammary carcinomas after three intermittent intratumoral (IT) injections.[18] This is the first STING agonist approaching into clinical trials jointly developed by Aduro and

Received: November 3, 2020
Published: January 20, 2021

Downloaded via BUTLER UNIV on May 16, 2021 at 05:45:03 (UTC).
See https://pubs.acs.org/sharingguidelines for options on how to legitimately share published articles.

ACS Publications

© 2021 American Chemical Society

https://dx.doi.org/10.1021/acs.jmedchem.0c01900
J. Med. Chem. 2021, 64, 1649−1669

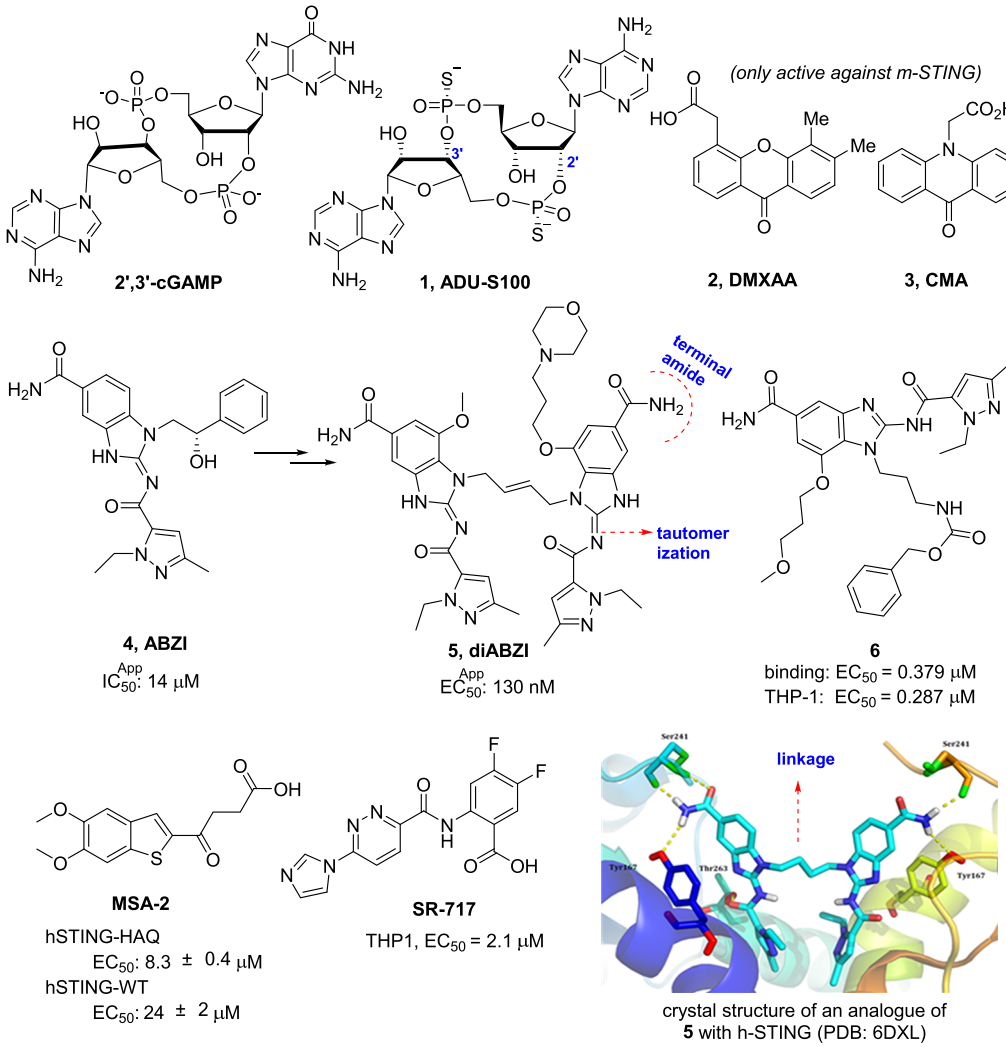

Figure 1. Representative STING agonists and our optimized hotspots (in blue color).

Novartis.[19,20] Unfortunately, Novartis recently terminated its clinical trials based on the marginally clinical responses either on monotherapy or in combination with PD-1 antibody spartalizumab.[20] Many other low-weight small-molecule STING agonists have also been reported,[16] however, most with distinct species specificity between human and mouse STING. For example, 5,6-dimethylxanthenone-4-acetic acid (**2**, DMXAA)[21,22] and 10-carboxymethyl-9-acridanone (**3**, CMA)[23] are the very early low-weight small-molecule STING agonists, but they are only active for m-STING, other than for h-STING.

Recently, Ramanjulu and co-workers[24] at GlaxoSmithKline reported a small-molecule STING agonist **4** (Figure 1) bearing a key amidobenzimidazole (ABZI) component and showing reproducible inhibition against ^{3}H-cGAMP binding to STING with an apparent inhibitory constant (IC_{50}^{APP}) of 14 μM. The crystal structure of this compound in complex with the h-STING C-terminal domain indicates that **4** binds in the same binding pocket of the endogenous ligand cGAMP, with each of two molecules of **4** bound with one STING subunit without contacts with each other. Subsequently, these authors used a linkage strategy to connect two molecules of **4** to form a dimer. After further modification, compound **5** (diABZI) was identified to exhibit a synergic effect in human peripheral blood mononuclear cells by inducing STING activation and subsequent secretion of IFN-β with an value of EC_{50}^{app} 130 nM. Different from CDNs (e.g., compound **1**), dimeric **5** can be administered intravenously (iv), and intermittent dosing of **5** at 1.5 mg/kg in subcutaneous CT26 tumors results in significant tumor growth inhibition and improved survival. At the end of 2019, Wang and co-authors[25] reported a procedure to optimize the amidobenzimidazole monomer and identified a lead compound **6** with improved biochemical and cellular potency, but the in vivo antitumor efficacy was modest. Very recently, Addona and co-workers[26] at Merck reported an orally available STING agonist MSA-2 (Figure 1), which has the potential to target the acidic tumor microenvironment. In the meantime, Lairson and co-workers[27] at Scripps reported a small-molecule STING agonist SR-717, which can be administered intraperitoneally.

Despite the structural novelty and significant antitumor efficacy of the dimeric compound **5**, limited structure−activity relationship (SAR) study has been reported. In this regard, we conducted a structural elaboration on this dimeric scaffold by modifying several hotspots of compound **5**, including the readily tautomeric *N*-acyl 1*H*-imidazol-2(3*H*)-imine component, the polaric terminal amido moiety, and the linkage (marked in blue in Figure 1). This approach led to identification of a new lead compound with improved safety profile, good systemic plasma exposure, and high antitumor

https://dx.doi.org/10.1021/acs.jmedchem.0c01900
J. Med. Chem. 2021, 64, 1649−1669

Scheme 1. Synthesis of Compounds 16−19 and 21 and 22[a]

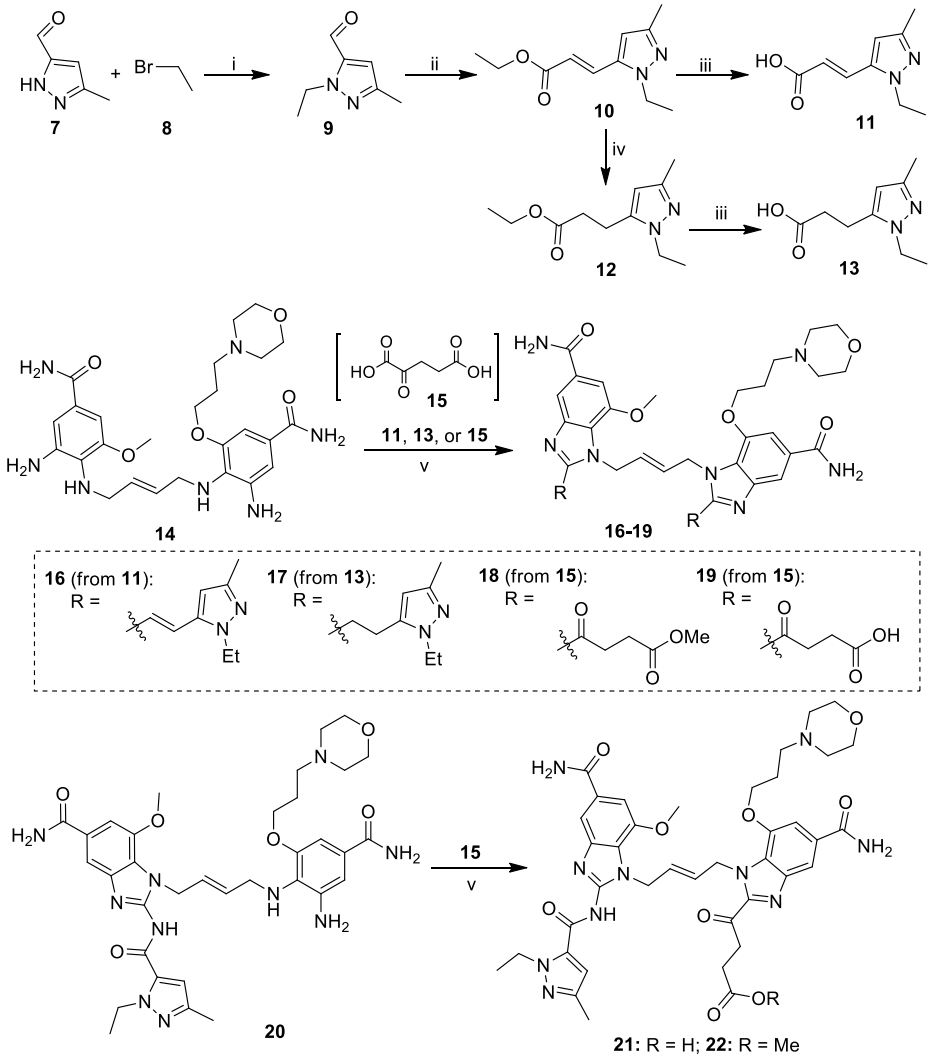

[a]Reactions and conditions: (i) Cs_2CO_3, DMF, and rt; (ii) ethyl 2-(diethoxyphosphoryl)acetate, NaH, DMF, and 0 °C to rt; (iii) LiOH·H_2O, MeOH/H_2O (1:1), and rt; (iv) 5% Pd/C, H_2, MeOH, and rt; and (v) for **16** and **17**: (1) EDCI, HOBt, DIPEA, DMF, and rt and (2) AcOH and 90 °C; for **18**: 4 N HCl aqueous solution, MeOH, and 100 °C; and for **19**: 4 N HCl aqueous solution, H_2O, and 100 °C.

activity. Herein, we describe our synthesis and biological characterization of these new STING agonists.

RESULTS AND DISCUSSION

Chemistry. The synthesis of compounds **16−19** and **21** and **22** bearing at least one flexible chain to replace the terminal pyrazole-5-carboxamide component is shown in Scheme 1. The intermediate **9** was obtained in 55% yield by alkylation of 3-methyl-1*H*-pyrazole-5-carbaldehyde (**7**) with bromoethane (**8**). The subsequent Horner−Wadsworth−Emmons reaction of intermediate **9** with triethyl phosphonoacetate delivered intermediate **10** in 44% yield. Hydrolysis of ester **10** using LiOH·H_2O afforded acrylic acid **11** in 49% yield. Hydrogenation of **10** led to intermediate **12** in 84% yield, which was then hydrolyzed to provide propanoic acid **13** in 76% yield. Condensation of the intermediate **14**, prepared according to a literature procedure,[24] with acids **11**, **13**, or 2-oxopentanedioic acid (**15**) was sluggish, and the corresponding products **16−19** were obtained in 13−21% overall yields. It is of note that different solvents affected the formation of compounds **18** and **19**. The reaction with water as the solvent gave carboxylic acid derivative **19**, whereas using MeOH as the solvent gave ester derivative **18**. Likewise, a similar event occurred in the preparation of compounds **21** and **22**.

The key intermediates **29a−29e** were synthesized as described in Scheme 2. Iodination of commercially available 2-methoxy-6-nitroaniline (**23**) with I_2 afforded **24** in 71% yield. Diazotization of **24** followed by chlorination led to intermediate **25** in 88% yield. Cu-catalyzed Sonogashira coupling of iodide **25** with trimethylsilylacetylene yielded **26** in 64% yield. Subsequent deprotection delivered **27a** in 93% yield. By following a similar literature procedure,[24] **27a−27d** were treated with *tert*-butyl (*E*)-(4-aminobut-2-en-1-yl)-carbamate affording **28a−28d** in 26−52% yields, respectively. The click reaction of **28a** with 1-azido-2-(2-methoxyethoxy)-ethane yielded **29a** in 52% yield. In the meantime, preparation of intermediate **29b** was achieved by treating **28b** with 2,2-dimethoxyethan-1-amine in 56% yield. Treating **28c** with DMF-DMA or 1,1-dimethoxy-*N*,*N*-dimethylethan-1-amine gave corresponding methylene benzamide derivatives, which were then subjected to cyclization with hydrazine acetate to afford compounds **29c** and **29d** in 64 and 49% yields,

https://dx.doi.org/10.1021/acs.jmedchem.0c01900
J. Med. Chem. 2021, 64, 1649−1669

Scheme 2. Synthesis of Intermediates 29a−29e[a]

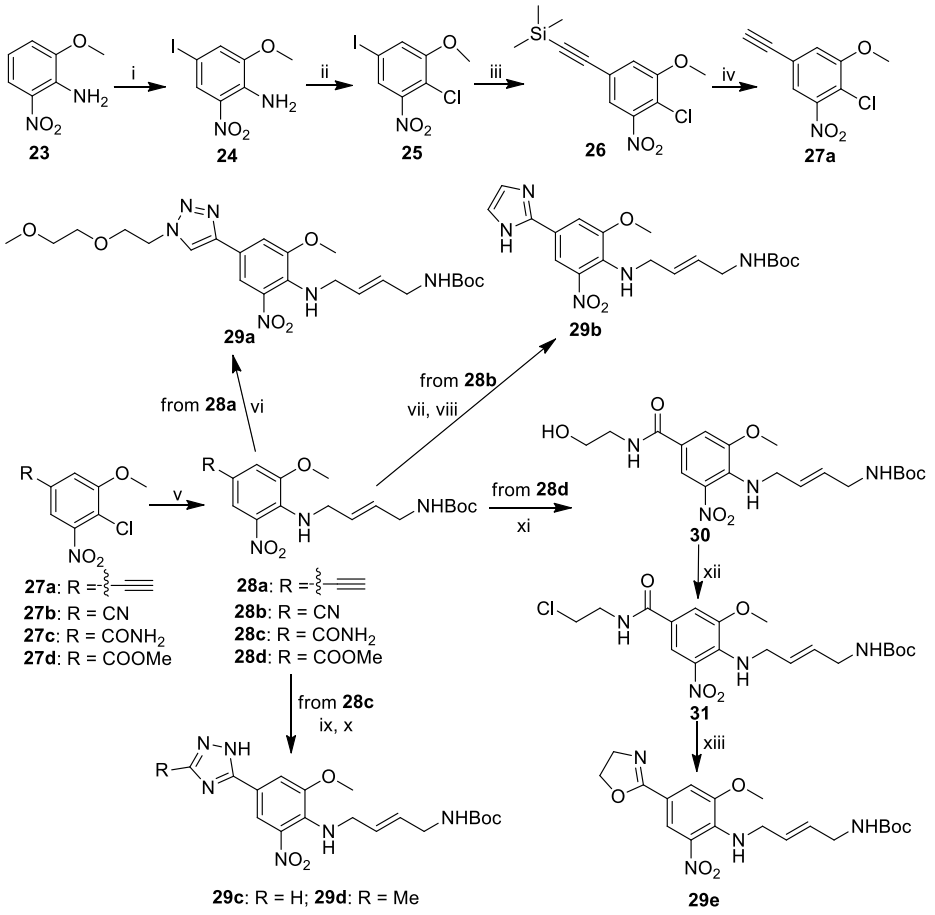

[a]Reactions and conditions: (i) I_2, Ag_2SO_4, EtOH, and rt; (ii) $TsOH·H_2O$, $NaNO_2$, CuCl, MeCN, H_2O, and 0 °C to rt; (iii) ethynyltrimethylsilane, $PdCl_2(PPh_3)_2$, CuI, DIPEA, THF, and 0 °C to rt; (iv) K_2CO_3, MeOH, and rt; (v) *tert*-butyl (*E*)-(4-aminobut-2-en-1-yl)carbamate, DIPEA, EtOH, 120 °C, and sealed tube; (vi) for **29a**: 1-azido-2-(2-methoxyethoxy)ethane, sodium ascorbate, $CuSO_4·5H_2O$, *t*-BuOH/H_2O = 2:1, and rt; for **29b**: 2-azidoethan-1-ol, sodium ascorbate, $CuSO_4·5H_2O$, *t*-BuOH/H_2O = 2:1, rt; (vii) NaOMe, MeOH, and rt; (viii) 2,2-dimethoxyethan-1-amine, AcOH, and 50 °C; (ix) for **29d**: DMF-DMA and 100 °C; for **29e**: 1,1-dimethoxy-*N*,*N*-dimethylethan-1-amine, 100 °C; (x) hydrazine acetate, EtOH, and 50 °C; (xi) 2-aminoethan-1-ol, MeOH, and 70 °C; (xii) $SOCl_2$, DCM, and 0 °C to rt; and (xiii) $NaHCO_3$, H_2O, and 0 °C to rt.

respectively.The ammonolysis reaction of ester **28d** with 2-aminoethan-1-ol produced amide **30** in 85% yield, which was then chlorinated with $SOCl_2$ followed by cyclization under a basic condition to deliver **29e** in 45% overall yield over two steps.

Dehydration of **32a** with $POCl_3$ afforded **32b** in 82% yield. The intermediates **32c** and **32d** were obtained by following similar procedures to those for preparation of **29b** and **29c** in 58 and 72% yields, respectively (Scheme 3). Substitution of **29a−29e** with **32a−32d** produced **33a−33l** in 31−50% yields. Reduction of the nitro group in **33a−33l** followed by imidazole ring fusion using 1-ethyl-3-methyl-1*H*-pyrazole-5-carbonyl isothiocyanate was conducted by following a literature procedure.[24] The dimeric compounds **34−45** were obtained in 27−42% yields over two steps.

As described in Scheme 4, compound **48** was obtained by a procedure similar to that for preparation of compounds **34−45**. It has to be mentioned that the same synthetic route was not suitable for synthesis of compounds **55** and **56**. Instead, the intermediate **50** needs to be prepared first. Reduction of **49** with sodium dithionite followed by treating with 1-ethyl-3-methyl-1*H*-pyrazole-5-carbonyl isothiocyanate in the presence of EDCI and Et_3N achieved compound **50**. Subsequent deprotection of **50** followed by substitution with halogenated compounds **51** and **52** yielded compounds **53** and **54** in 41 and 38% overall yields, respectively. The target products **55** and **56** were prepared in 25 and 31% yields, respectively, by following literature procedures.[24] Dimeric compounds **64−66** with structural modifications on the linker were implemented as shown in Scheme 5 by following similar procedures as described above.

Activation of New Compounds on Both h- and m-STING. To quickly identify potent STING agonists for further study, we first determined activation folds of new compounds against h- and m-STING by respectively measuring the secreted embryonic alkaline phosphatase (SEAP) reporter of interferon-stimulated gene (ISG) in human THP1-Blue-ISG cells and the secreted luciferase reporter of ISG in mouse RAW-Lucia cells, compared to the control. In our initial experiments, we found that compound **5** (diABZI) is more sensitive for h-STING and less sensitive for m-STING. Therefore, we screened the activation potency of new compounds by treating with human THP1-Blue-ISG cells at a concentration of 10 μM whereas with mouse RAW-Lucia cells at higher concentrations of 50 μM.

https://dx.doi.org/10.1021/acs.jmedchem.0c01900
J. Med. Chem. 2021, 64, 1649−1669

Scheme 3. Synthesis of Compounds 34−45[a]

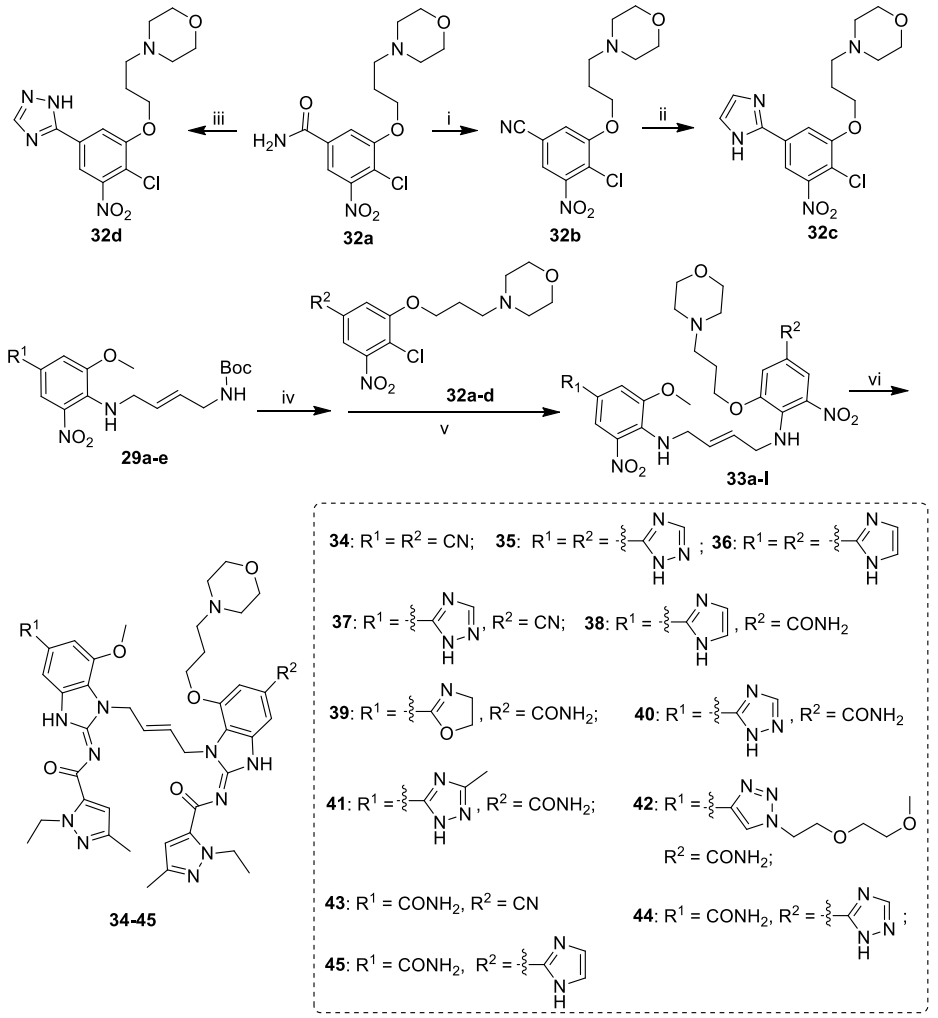

[a]Reactions and conditions: (i) $POCl_3$ and 100 °C; (ii) NaOMe, MeOH, and rt and then 2,2-dimethoxyethan-1-amine, AcOH, and 50 °C; (iii) DMF-DMA and 100 °C and then hydrazine acetate, EtOH, and 50 °C; (iv) 4 N HCl in 1,4-dioxane, MeOH, and rt; (v) DIPEA, *i*-PrOH, 120 °C, sealed tube, and 2 days; and (vi) (a) $Na_2S_2O_4$, $NH_3{\cdot}H_2O$, THF/H_2O = 1:1, and rt and (b) 1-ethyl-3-methyl-1*H*-pyrazole-5-carbonyl isothiocyanate, EDCI, Et_3N, DMF, and 0 °C to rt.

As shown in Table 1, we first tested compounds from modification of the readily tautomeric pyrazole-5-carboxamide component of compound **5** by changing the amido linkage with an ethylenyl or ethyl moiety. The resulting compounds **16** and **17** showed no activation against both h- and m-STING with activation fold less than 1.0 compared to the control, whereas the reference compound **5** showed approximately 26-fold and 8-fold activation against h-STING (10 μM) and m-STING (50 μM), respectively. Interestingly, compound **18** bearing a 3-(methoxycarbonyl)propionyl moiety to replace the pyrazole-5-carboxamide component of **5** retained significant activation in the human THP1-Blue-ISG cells with an activation fold of 6.16; however, nearly no activation was observed in the mouse RAW-Lucia cell. Compound **19**, bearing terminal carboxylic groups in the tails of the dimer, retained a similar activation fold against h-STING (9 fold) but was still inactive against m-STING. Meanwhile, we selectively replaced one pyrazole-5-carboxamido edge and kept the other one intact, yielding acid **21** and ester **22**, respectively. Both compounds lost activation against both h- and m-STING. These results indicate that the two down-side pyrazole-5-carboxamido edges are not only important to the activation potency but also highly sensitive to different species.

Next, we modified the two up-side primary amide moieties of **5** with the aim to reduce the polarity and increase stability. As shown in Table 2, replacement of the two amido functions with two cyano groups afforded compound **34**, which retained good activation against h-STING with an activation fold of 7.9 at 10 μM but showed no activation against m-STING at 50 μM. Conversion of the two amido moieties to heterocyclic triazole and imidazole motifs yielded compounds **35** and **36**, respectively, which showed distinct activation patterns. Triazole **35** showed significant activation against h-STING (4.9-fold) and no activation against m-STING. However, imidazole **36** only showed marginal activation for h-STING (1.22-fold) and no activation for m-STING. Interestingly, compound **37** carrying a triazole on one side and a cyano on the other side also showed strong activation against h-STING with an activation fold of 11.10, whereas the activation for m-STING was negligible.

Meanwhile, we also tested compounds with only one of the terminal amido groups in **5** replaced by other functional

https://dx.doi.org/10.1021/acs.jmedchem.0c01900
J. Med. Chem. 2021, 64, 1649−1669

Scheme 4. Synthesis of Compounds 48, 55, and 56[a]

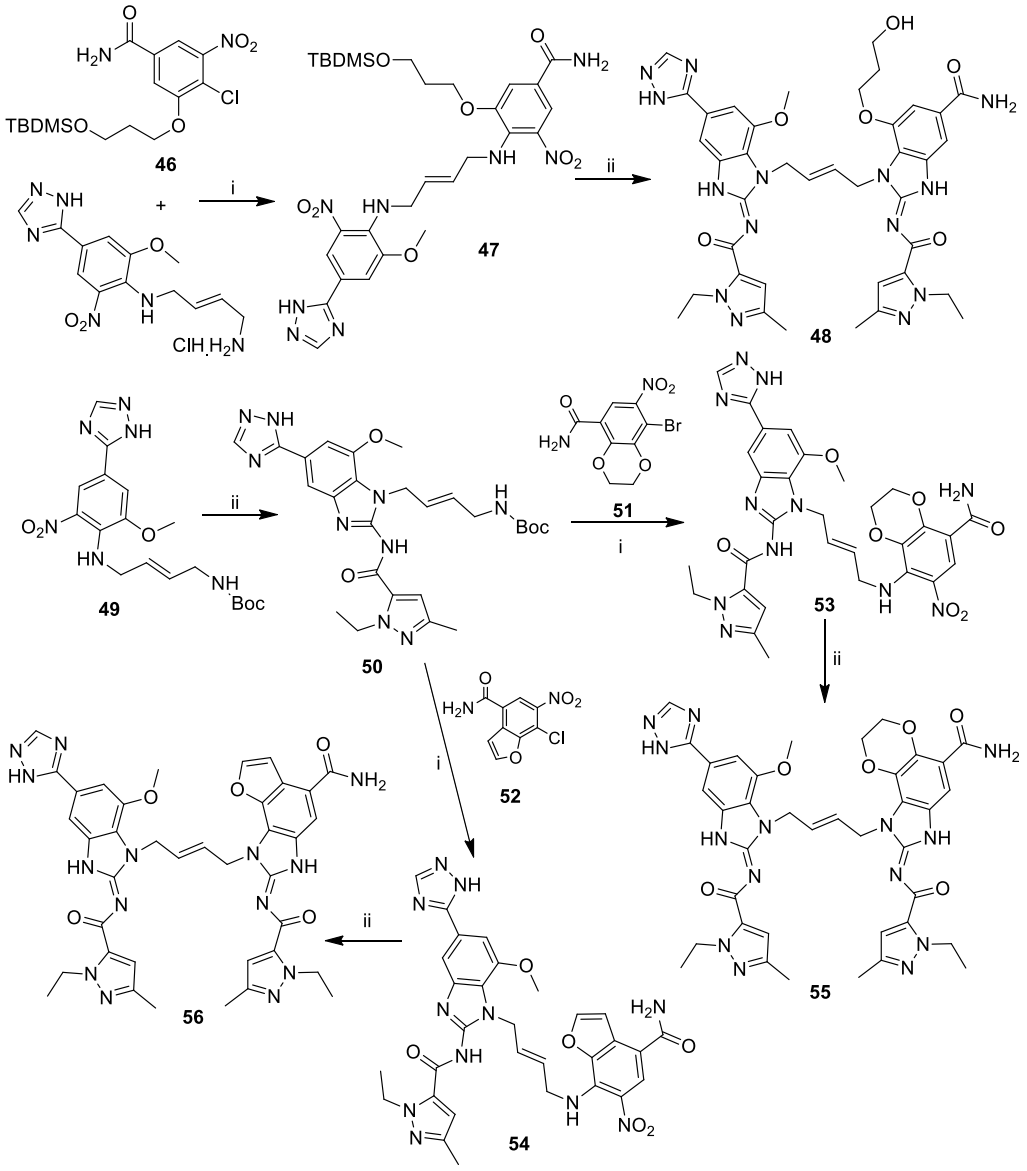

[a]Reactions and conditions: (i) DIPEA, *i*-PrOH, 120 °C, sealed tube, and 2 days; (ii) (a) $Na_2S_2O_4$, $NH_3{\cdot}H_2O$, THF/H_2O = 1:1, and rt; (b) 1-ethyl-3-methyl-1*H*-pyrazole-5-carbonyl isothiocyanate, EDCI, Et_3N, DMF, and 0 °C to rt; and (c) TBAF, AcOH, THF, and 0 °C to rt.

groups. As shown in Table 3, using a heterocycle to mask the left-side amido group but retain the H-bonding ability generated compounds **38**−**42**. All these analogues showed markedly high activation for h-STING with activation folds ranging between 17.25 and 19.21, whereas their activation for m-STING is moderate. Triazole **40** generated greater activation than imidazole **38** and dihydrooxazole **39** with activation folds of 19.21, 17.50, and 18.30, respectively, for h-STING, indicating that the triazole moiety can well mimic both H-bonding donor and acceptor properties of the amido motif. Importantly, compared to **38** and **39**, triazole **40** also showed modest activation for m-STING at both 50 μM with an activation fold of 3.20. Further substitution on the triazole moiety yielded compounds **41** and **42**, all retaining significant activation for h-STING with activation folds of 18.75 and 17.25, respectively; however, the activation for m-STING was reduced. As a comparison, we also kept the left-side amido moiety of compound **5** intact but replaced the right-side one, leading to compounds **43**−**45**. All three compounds still retained significant activation on h-STING with activation folds of 13.38−17.31; however, again, only the triazole **44** showed certain stimulation on m-STING with an activation fold of 2.17 at 50 μM.

Since triazoles **40** and **44** are able to activate both h- and m-STING, we further optimized this compound by incorporating aqueous substituents or replacing the but-2-ene linker with other variations. As shown in Table 4, introducing a water soluble hydroxypropyl chain delivered compound **48**, which retained significant activation on h-STING with an activation fold of 16.66; however, no activation was observed on m-STING. Fusing 1,4-dioxane to the benzamide component led to compound **55**, which nearly completely lost the activation effects on both h- and m-STING. Notably, compound **56** obtained by fusing a furan moiety to the benzamide component exhibited high activation on h-STING with an activation fold of 17.04; unfortunately, no obvious activation

https://dx.doi.org/10.1021/acs.jmedchem.0c01900
J. Med. Chem. 2021, 64, 1649−1669

Scheme 5. Synthesis of Compounds 64−66[a]

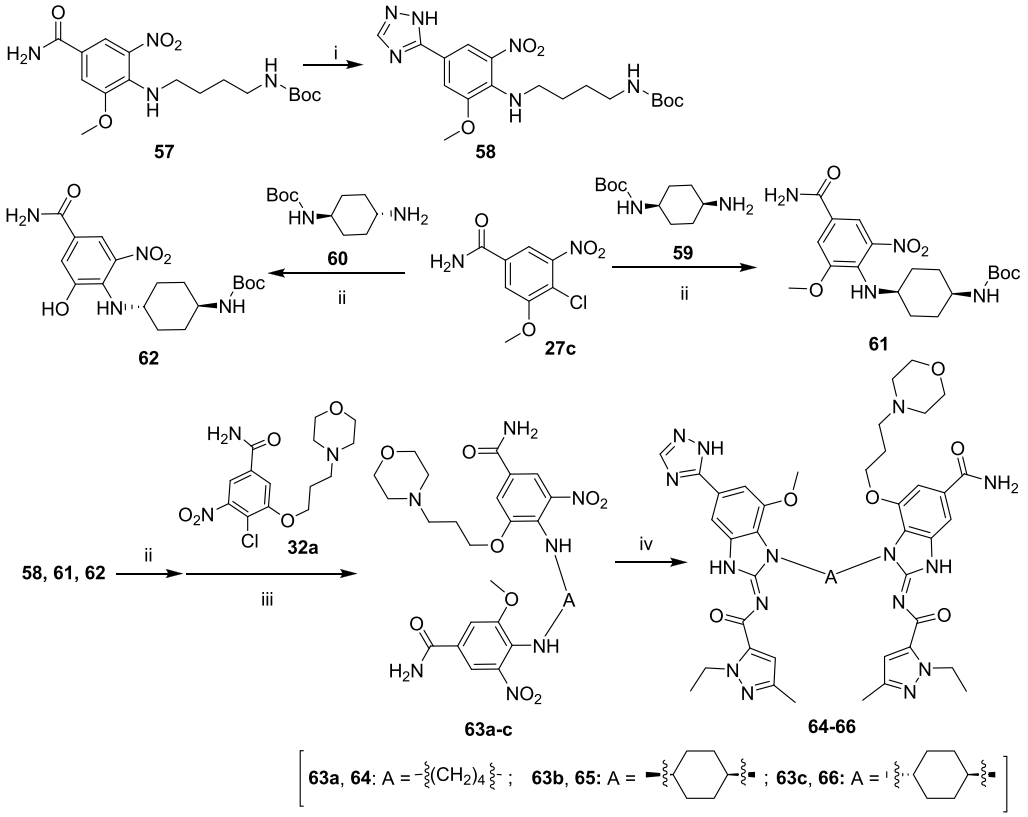

[a]Reactions and conditions: (i) (a) DMF-DMA and 100 °C and (b) hydrazine acetate, EtOH, and 50 °C; (ii) 4 N HCl in 1,4-dioxane, MeOH, and rt; (iii) DIPEA, EtOH, sealed tube, and 120 °C; (iv) DIPEA, *i*-PrOH, 120 °C, sealed tube, and 2 days; and (v) (a) $Na_2S_2O_4$, $NH_3{\cdot}H_2O$, THF/H_2O = 1:1, and rt and (b) 1-ethyl-3-methyl-1*H*-pyrazole-5-carbonyl isothiocyanate, EDCI, Et_3N, DMF, and 0 °C to rt.

on m-STING was observed. Switching the but-2-ene linkage to butyl or cyclohexyl afforded compounds **64−66**; however, all showed marginal activation on both h- and m-STING.

EC_{50} Values of Selected Compounds against Both h- and m-STING. With the preliminary data above, we further tested the compounds that showed obvious stimulatory effects on h- and/or m-STING at various concentrations and calculated their EC_{50} values on h-STING or m-STING by measuring the secreted luciferase reporter of interferon-stimulated gene (ISG) in human THP1-Dual cells and mouse RAW-Lucia cells, respectively. As shown in Table 5, compound **5** is extremely potent for h-STING with an EC_{50} value less than 0.1 nM, whereas the activation potency for m-STING is modest by showing an EC_{50} value of 3.0 μM. Compounds **18**, **34**, and **37**, in which both the two down-side pyrazole-5-carboxamide components or the two up-side benzamido moieties were replaced, showed reduced activation effects with EC_{50} values of 29.1, >50, and 26.0 μM, respectively, for h-STING, and there is no activation for m-STING (EC_{50} > 50 μM). Imidazole **38**, dihydrooxazole **39**, and methyl triazole **41** all showed modest potency on h-STING with EC_{50} values of 3.28, 1.54, and 2.55 μM, respectively; however, they were inactive on the m-STING. In parallel to the preliminary results, triazole **40** showed a high activation effect on the h-STING, with an EC_{50} value of 0.24 μM, only slightly less potent than compound **5**. To be glad, this compound showed somewhat activation on the m-STING, although the activation potency is rather modest with an EC_{50} value of 39.51 μM.

Among the right-side amido-replacing analogues, triazole **44** remains as more potent than nitrile **43** and imidazole **45** with EC_{50} values of 0.33, 1.02, and 0.79 μM, respectively, but triazole **44** is less potent than the triazole **40** (0.33 vs 0.24 μM). Compounds **43** to **45** showed negligible potency on m-STING with EC_{50} values greater than 50 μM. The analogues **48** and **66** showed much less activation effects at both h- and m-STING.

From the results above, triazole **40** turns out as the most potent STING activator with EC_{50} values of 0.24 and 39.51 μM for h- and m-STING, respectively. This compound is less potent than compound **5**; however, in view of the well-accepted drug-like properties and safety profile of triazole compounds in drug discovery, compound **40** was selected for further profiling, side-by-side with the reference compound **5**. Meanwhile, a docking study was also conducted (Figures S1 and S2, see the Supporting Information). It was found that the triazole moiety in compound **40** is an excellent substituent for the amido group of compound **5**. This component forms a hydrogen bond at the top with Ser241 and has a $\pi-\pi$ interaction with Try240. The nitrogen atom in the pyrazole ring forms a new hydrogen bond with Ser162. This result partially rationalizes the high potency of the triazole **40**.

Pharmacokinetic Properties and Aqueous Solubility Study of Compound 40. Since the CDN analogues, such as 2′,3′-cGAMP and ADU-S100, are mainly administered by intratumoral (IT) administration, therefore, we first tested the pharmacokinetic (PK) properties of triazole compound **40** in rats. As shown in Table 6, compound **40**, in comparison to

https://dx.doi.org/10.1021/acs.jmedchem.0c01900
J. Med. Chem. 2021, 64, 1649−1669

Table 1. Activation Folds of New Compounds against m- and h-STING[a]

Compound	Structure	Fold (h-STING) (10 μM)	Fold (m-STING) (50 μM)
5	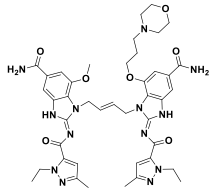	25.96	8.11
16	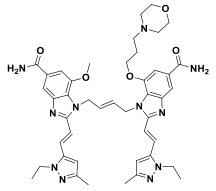	0.98	0.96
17	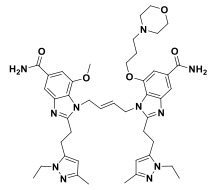	0.95	0.90
18	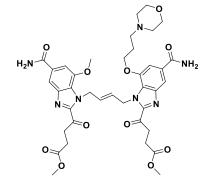	6.16	1.01
19	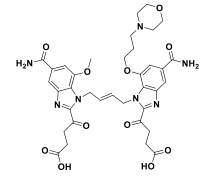	9.00	1.40
21	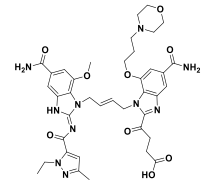	0.86	0.93
22	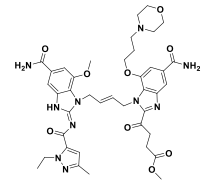	0.83	0.90

[a]Data were the average values of at least two repeated experiments.

compound **5**, shows an overall similar PK profile in rats at 1 mg/kg iv injection, with a slightly higher plasma exposure (678 vs 657 h ng/mL) and slightly lower clearance (23.9 vs 26 mL/min/kg).

In the meantime, we also tested the aqueous solubility of compounds **40** and **5** by conversion to their corresponding hydrochloride salts. As shown in Table 7, compared to the modest solubility of **5**, the HCl salt form of compound **40** is completely aqueously soluble and its solubility is >20-fold higher than that of the HCl salt form of **5** (71.33 vs 3.23 mg/L). In addition, despite the high loading of the N atom, both compounds showed no obvious hERG inhibition with IC_{50} values greater than 40 μM, indicating their negligible cardiac toxicity.

Compound 40 Potently Activated the STING Signaling. The THP1-Dual cell bearing both the ISG reporter and NF-κB reporter was used to determine the activation of compound **40** on STING signaling. As shown in Figure 2A,B, compound **40** dramatically activated the ISG signaling and NF-κB signaling in a dose-dependent manner. The reference compound **5** also showed high potency for both signaling processes; however, a dose-dependent manner is not obvious. Next, we determined the cytokine secretion of THP1-Dual cells under treatment with compound **40** or **5**. As expected, both compounds dramatically increased the secretion of IP-10 and IFN-β at tested concentrations (Figure 2C,D). At a high concentration of 10 μM, compounds **5** and **40** exhibited similar high potency on IP-10 and IFN-β secretion, while at lower concentrations (0.1 and 0.01 μM), compound **5** showed more potency on IP-10 secretion than **40**.

Meanwhile, the STING downstream signaling proteins were assessed as well after treatment with compound **40** or **5** for 4 h. As shown in Figure 2E, both compounds remarkably increased the phosphorylation of the TBK1/IRF3 signaling pathway in a dose-dependent manner, demonstrating the activation of STING signaling by the two compounds. Furthermore, the STING-knockout THP1-Dual cells (THP1-Dual-KO-STING) were used to evaluate the specificity of compounds. Treatment with this cell showed that knockout of STING completely blocked the activation on ISG signaling (Figure 2F), indicating the specificity of both compounds **40** and **5** on the STING signaling.

Compound 40 Directly Activated Human STING Isoforms and Mouse STING. To confirm whether compound **40** could directly target on STING protein, we used the differential scanning fluorimetry (DSF) assay to test the binding of this compound on various human STING isoforms and mouse STING. As shown in Figure 3A−E, the T_m value of the melt curve was increased after treatment with compound **40** as compared to the vehicle, similar to that of the positive control **5**. The melt curve shifted to higher temperature, indicating that compounds **40** and **5** can directly bind and stabilize human STING protein isoforms,[29] including hSTING-R232, hSTING-H232, hSTING-293Q, and hSTING-AQ, as well as mouse wild-type STING protein R231. Combining these findings with the previous results on THP1-Dual cells bearing STING isoform of HAQ, we concluded that compound **40** has the capacity of activating all the five main STING isoforms. In addition, the binding ability of compounds **40** and **5** to human wild-type STING

https://dx.doi.org/10.1021/acs.jmedchem.0c01900
J. Med. Chem. 2021, 64, 1649−1669

Table 2. Activation Folds of Compounds against h- and m-STING[a]

Compound	Structure	Fold (h-STING) (10 μM)	Fold (m-STING) (50 μM)
34	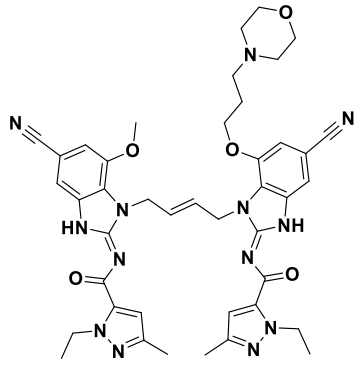	7.90	1.16
35	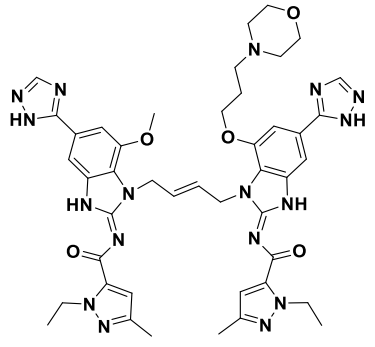	4.90	1.18
36	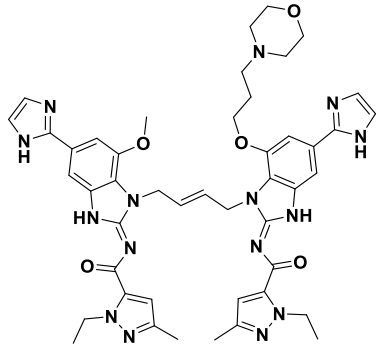	1.22	1.21
37	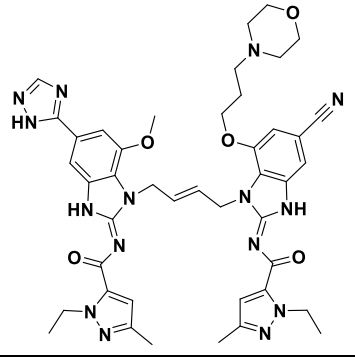	11.10	1.34

[a]Data were the average values of at least two repeated experiments.

(R232) was determined using a commercial competition assay kit by homogeneous time-resolved fluorescence (HTRF) technology. Compound **40** has an EC_{50} value of 6.2 nM, compatible to the endogenous ligand 2′,3′-cGAMP (5.8 nM),

https://dx.doi.org/10.1021/acs.jmedchem.0c01900
J. Med. Chem. 2021, 64, 1649−1669

Table 3. Activation Folds of Compounds against h- and m-STING[a]

Compound	Structure	Fold (h-STING) (10 μM)	Fold (m-STING) (50 μM)
38	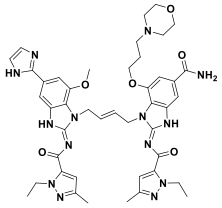	17.50	1.42
39	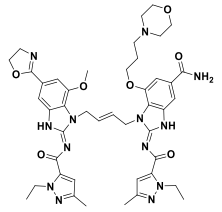	18.33	0.99
40	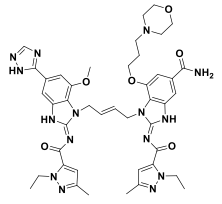	19.21	3.20
41	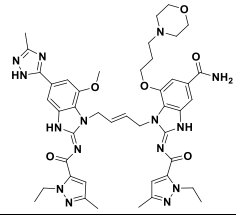	18.75	0.92
42	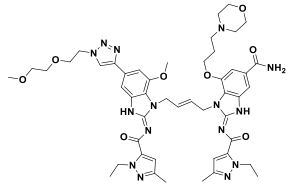	17.25	1.16
43	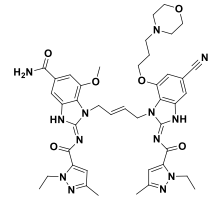	13.80	1.07
44	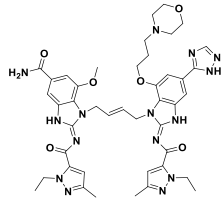	17.00	2.17
45	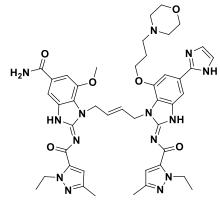	17.31	1.18

[a]Data were the average values of at least two repeated experiments.

while the EC_{50} value of compound **5** was extremely low (<0.1 nM) (Figure S3, see the Supporting Information). To further determine the activation of this compound on different STING isoforms, we used 293-Dual-hSTING-R232 cells and 293-Dual-hSTING-H232 cells to determine its activation on hSTING-R232 and hSTING-H232, respectively. The results showed that compound **40** potently activated ISG signaling in a dose-dependent manner in both two reporter cells (Figure 3F,G), while compound **5** exhibited high activity as well on hSTING-R232 and hSTING-H232 but without an obvious dose-dependent manner. In addition, activation of compound **40** on mouse STING protein was also tested using both RAW-Lucia and RAW-Lucia-KO-STING cells. Interestingly, although compound **40** is 13-fold less potent than compound **5** against m-STING with EC_{50} values of 39.51 and 3 μM, respectively (Table 5), both compounds dramatically activated the ISG signaling in RAW-Lucia cells. Further, no activity was observed in RAW-Lucia-KO-STING cells (Figure 3H), demonstrating compound **40** specifically targeted on mouse STING signaling.

Antitumor Activity of Compound 40 in Animal Models. To evaluate whether the observed immune activating effect of compound **40** in cells can transform to potent antitumor activity in vivo, mice models bearing orthotopic transplanted breast tumor (4T1) or subcutaneous transplanted colon tumor (CT26) were used for study. First, BALB/c mice bearing orthotopic 4T1 tumors were intravenously (iv) received comparable dose of compound **40** or **5** at 10 mg/kg at days 1, 4, and 7. Compound **40** was found to dramatically suppress the tumor growth as compared to the vehicle control (Figure 4A). Although compound **5** was found more potent and induced tumor regression, unfortunately, high toxicity was observed and all the tested mice were dead after the third injection, indicating that a lower dose should be used for compound **5** to avoid potential overdose toxicity.[24] Compound **40** was well tolerated, although slight weight loss was observed after the third injection but mice were recovered well afterward (Figure 4B).

Moreover, we also tested the effects of both compounds on the CT26 colon tumor model by intratumoral (IT) injection at days 1, 4, and 7, using the widely used m-STING specific agonist **2** (DMXAA, Figure 1) as a comparison. As shown in Figure 4C, compounds **40** and **2** both inhibited CT26 tumor growth significantly. The effect of **2** is more sustained than that of **40**. The IT injection of both compounds was well tolerated as assessed by body weight (Figure 4D). These results demonstrated that compound **40** is well tolerated and exerts potent antitumor efficacy in allograft tumor models of mice.

CONCLUSIONS

In summary, activation of STING by agonists has emerged as an exciting strategy of IO therapy for cancer; however, the first-

https://dx.doi.org/10.1021/acs.jmedchem.0c01900
J. Med. Chem. 2021, 64, 1649−1669

Table 4. Activation Folds of Triazole Analogues against h- and m-STING[a]

Compound	Structure	Fold (h-STING) (10 μM)	Fold (m-STING) (50 μM)	Compound	Structure	Fold (h-STING) (10 μM)	Fold (m-STING) (50 μM)
48	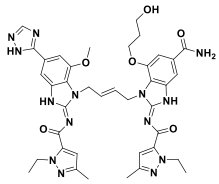	16.66	0.96	**64**	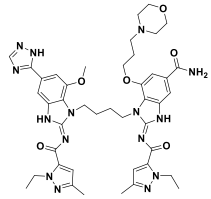	1.28	1.20
55	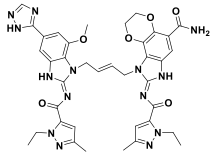	1.58	1.10	**65**	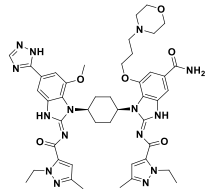	1.14	0.59
56	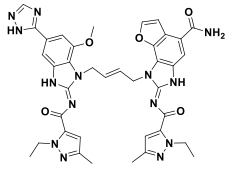	17.04	1.14	**66**	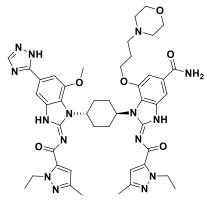	3.86	0.48

[a]Data were the average values of at least two repeated experiments.

Table 5. EC_{50} Values of Selected Compounds against Both h- and m-STING[a]

compound	EC_{50}, μM (h-STING)	EC_{50}, μM (m-STING)
5 (diABZI)	<0.0001	3.00 ± 1.44
18	29.10 ± 4.52	>50
34	>50	>50
37	26.0 ± 8.86	>50
38	3.28 ± 0.10	>50
39	1.54 ± 0.46	>50
40	0.24 ± 0.03	39.51 ± 9.85
41	2.55 ± 0.27	>50
43	1.02 ± 0.22	>50
44	0.33 ± 0.05	>50
45	0.79 ± 0.04	>50
48	2.66 ± 0.13	>50
66	>50	>50

[a]Data were the average values of at least two repeated experiments.

generation STING agonists, (CDN) analogues, have met multiple limitations. Therefore, low-weight non-CDN small-molecule STING agonists are urgently needed. To take advantage of the unique dimeric structure of the high potency STING agonist **5** (diABZI) bearing two amidobenzimidazole motifs, we conducted a structural elaboration by modifying several structural hotspots of this dimeric scaffold, including the readily tautomeric *N*-acyl 1-ethyl-3-methyl-1*H*-pyrazole-5-imino component, the polaric terminal amido moiety, and the linkage. Several series of analogues were synthesized, and their SAR was evaluated against both h- and m-STING. All these compounds were found generally equally sensitive for h-STING but much less effective for m-STING. Triazole **40** was found as the most potent STING activator with EC_{50} values of 0.24 and 39.51 μM for h- and m-STING, respectively. This compound possesses a slightly better PK profile and is >20-fold more aqueously soluble than the reference compound **5** both in their HCl salt form. Activation of the STING signaling by compound **40** was evidenced in the THP1-Dual cell bearing both the ISG reporter and NF-kB reporter. Treatment with this compound was found to dramatically promote secretion of IP-10 and IFN-β and increase the phosphorylation of STING downstream TBK1/IRF3 signaling pathway in THP1-Dual cells, whereas similar activation was not observed in the STING-knockout cells. Further, compound **40** was found to

Table 6. Pharmacokinetic Parameters of Compound 40[a]

	iv (1 mg/kg)					
compound	$T_{1/2}$ (h)	AUC_{last} (h ng/mL)	AUC_{INF_obs} (h ng/mL)	$CL_{\_obs}$ (mL/min/kg)	MRT_{INF_obs} (h)	V_{ss_obs} (mL/kg)
5	1.14	657	666	26	0.633	965
40	0.697	678	705	23.9	0.503	722

[a]Values are the average of three runs. Vehicle: po, DMSO/0.5% HPMC (5/95, v/v); iv, EtOH/PEG300/NaCl (10/40/50, v/v/v); CL, clearance; V_{ss}, volume of distribution; $T_{1/2}$, half-life; and AUC, area under the plasma concentration time curve.

https://dx.doi.org/10.1021/acs.jmedchem.0c01900
J. Med. Chem. 2021, 64, 1649−1669

Table 7. Aqueous Solubility and hERG Inhibition of Compound 40[a]

	standard aqueous solution		saturated aqueous solution		
compound	concentration (mg/mL)	area (mAU s)	area (mAU s)	solubility (mg/mL)	hERG (IC_{50}, μM)
HCl salt of **5**	2.26	1.96212×10^4	2.8048×10^4	3.23	>40
HCl salt of **40**	4.81	4.7300×10^4	7.01476×10^5	71.33	>40

[a]Values are the average of three runs.

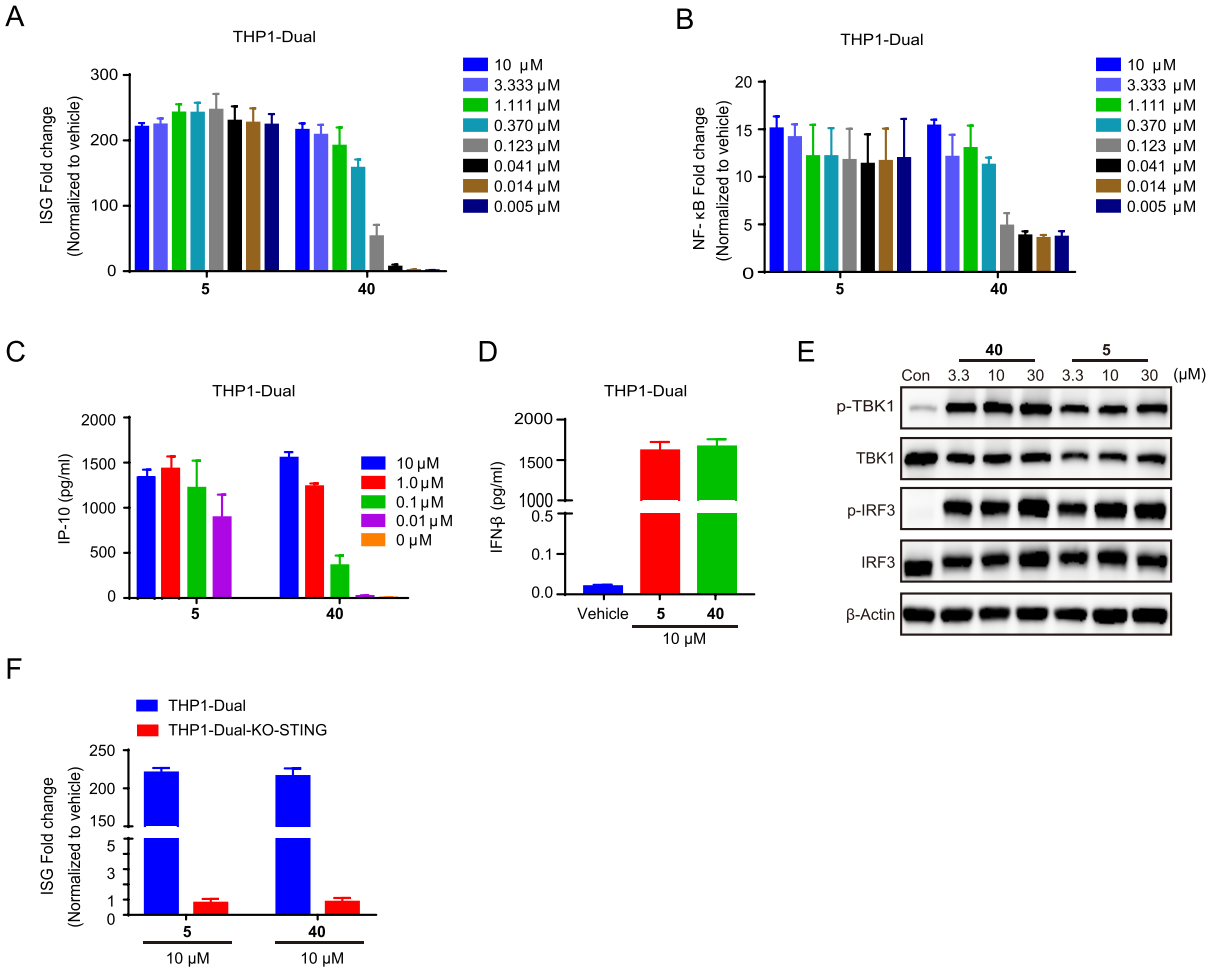

Figure 2. Compound **40** potently activated the STING signaling pathway. (A) Activation of compounds on the ISG reporter of THP1-Dual cells after 24 h treatment, fold change of activation was calculated to the vehicle control. (B) Activation of compounds on the NF-κB reporter of THP1-Dual cells after 24 h treatment, fold change of activation was calculated to the vehicle control. (C) IP-10 secretion of THP1-Dual cells under the treatment of compounds for 24 h. (D) IFN-β secretion of THP1-Dual cells under the treatment of compounds for 24 h. (E) THP1-Dual cells were treated with indicated compounds for 4 h and determined by immunoblotting. (F) Activity of compound on the ISG reporter in THP1-Dual and THP-Dual-KO-STING cells after 24 h treatment, fold change of activation was calculated to the vehicle control.

directly bind and stabilize all isoforms of human STING proteins, including hSTING-R232, hSTING-H232, hSTING-293Q, and hSTING-AQ, as well as mouse STING protein R231. In vivo, intermittent administration of **40** showed significant antitumor efficacy and good safety both in BALB/c mice bearing orthotopic 4T1 breast tumor and in CT26 colon tumor models.

EXPERIMENTAL SECTION

Chemical Reagents and General Method. All commercially available starting materials and solvents are reagent grade and used without further purification. Column chromatography was performed using 300−400 mesh or 200−300 mesh silica gel. Analytical TLC was carried out employing silica gel 60 F254 plates, and spots were visualized by UV (254 or 365 nm). ^{1}H and ^{13}C NMR spectra were recorded with a Varian Mercury 300 or 400 MHz NMR spectrometer. Chemical shifts (δ) were reported in ppm downfield from an internal TMS standard, and J values were given in Hz. Low- and high-resolution mass spectra were obtained in the ESI mode from an Elite mass spectrometer. Purity of final compounds was determined by analytical HPLC, which was carried out on an Agilent Technologies 1260 series LC system with ultraviolet wavelengths in UV 254. HPLC analysis conditions are as follows: XDB-C18, 3.5 μm, 4.6 mm × 150 mm, and H_2O/MeOH or H_2O/MeCN and 0.1% TFA or 0.1% DEA. All the assayed compounds showed a chemical purity of 95−100%.

Compounds **14** and **20** were prepared according to the literature procedures.[24,28]

*1-Ethyl-3-methyl-1H-pyrazole-5-carbaldehyde (**9**).* To a solution of compound **7** (550 mg, 5.0 mmol) and Cs_2CO_3 (2.44 g, 7.5 mmol) in DMF (10 mL) was added bromoethane (708 mg, 6.5 mmol) under a N_2 atmosphere. The mixture was stirred at room temperature for 2 h

https://dx.doi.org/10.1021/acs.jmedchem.0c01900
J. Med. Chem. 2021, 64, 1649−1669

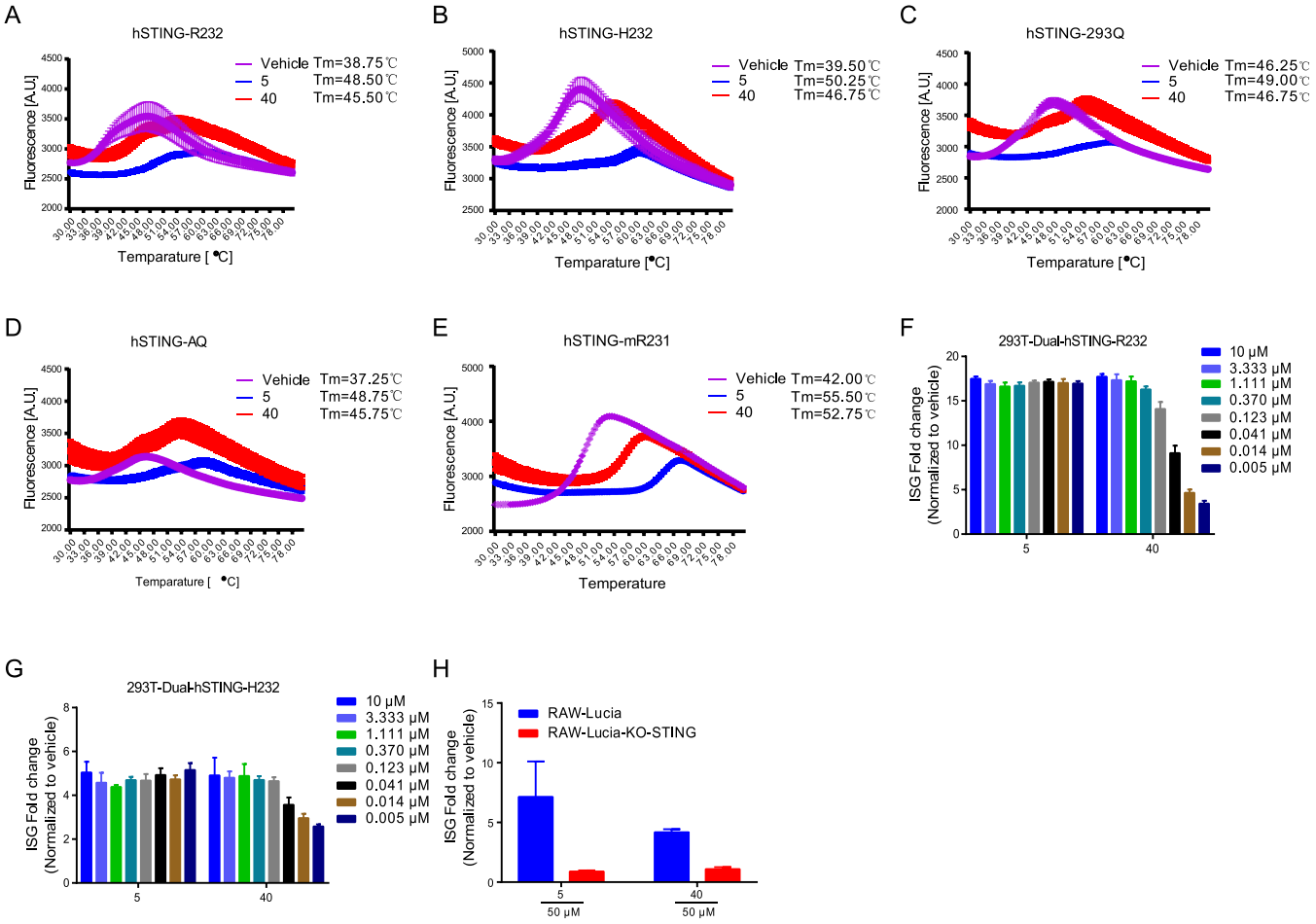

Figure 3. Compound **40** directly activated various h-STING isoforms and m-STING. (A–E) Binding of compounds on human STING isoform R232, human STING isoform H232, human STING isoform 293Q, human STING isoform AQ, and mouse STING R231 (WT), respectively, as measured by DSF, shown as the mean value and standard error of mean of the fluorescence, $n = 3$. (F, G) Activation of compound on the ISG reporter in 293T-Dual-hSTING-R232 and 293T-Dual-hSTING-H232 cells after 24 h treatment, fold change of activation was calculated to the control. (H) Activation of compound on the ISG reporter in RAW-Lucia and RAW-Lucia-KO-STING cells after 24 h treatment, fold change of activation was calculated to the control.

and then diluted with water (60 mL). After extraction with EtOAc (3 × 50 mL), the combined organic phase was washed with brine, dried over Na_2SO_4, filtered, and concentrated in vacuo. The residue was further purified by silica gel column chromatography to afford **9** (378 mg, 55%). ^{1}H NMR (400 MHz, $CDCl_3$): δ 9.87 (s, 1H), 6.52 (s, 1H), 4.15 (q, J = 7.3 Hz, 2H), 1.45 (t, J = 7.3 Hz, 3H).

*Ethyl (E)-3-(1-Ethyl-3-methyl-1H-pyrazol-5-yl)acrylate (**10**).* To a solution of compound **9** (348 mg, 2.5 mmol) and ethyl 2-(diethoxyphosphoryl)acetate (582 mg, 2.6 mmol) in DMF (10 mL) at 0 °C was added NaH (90 mg, 3.75 mmol). The mixture was stirred at room temperature overnight and then quenched with saturated NH_4Cl solution. After extraction with EtOAc (3 × 50 mL), the combined organic phase was washed with brine, dried over Na_2SO_4, filtered, and concentrated in vacuo. The residue was further purified by silica gel column chromatography to afford **10** (213 mg, 44%). ^{1}H NMR (400 MHz, DMSO): δ 7.42 (d, J = 16.0 Hz, 1H), 6.52 (s, 1H), 6.38 (d, J = 16.0 Hz, 1H), 4.16 (q, J = 7.1 Hz, 2H), 4.07 (q, J = 7.2 Hz, 2H), 2.27 (s, 3H), 1.30 (t, J = 7.2 Hz, 3H), 1.24 (t, J = 7.1 Hz, 3H).

*Ethyl 3-(1-Ethyl-3-methyl-1H-pyrazol-5-yl)propanoate (**12**).* To a solution of compound **10** (213 mg, 1.1 mmol) in MeOH (5 mL) was added 5% Pd/C (212 mg). After hydrogenation at room temperature for 8 h, the mixture was filtered and concentrated in vacuo to deliver a light yellow oil in 84% yield, which was then used in the next step without further purification.

General Procedure for Synthesis of Compounds 11 and 13. To a solution of compound **10** or **12** (1.0 mmol) in MeOH/H_2O (6 mL, 1:1) was added LiOH·H_2O (3 mmol). The mixture was stirred at room temperature for 2 h. The mixture was concentrated in vacuo. The residue was acidified with 1 N HCl aqueous solution and extracted with EtOAc. The combined organic phase was washed with brine, dried over Na_2SO_4, filtered, and concentrated in vacuo. The crude products **11** and **13** were obtained in 48–76% yields and used in the next step without further purification.

General Procedure for Synthesis of Compounds 16 and 17. The solution of compound **14** (0.1 mmol), EDCI (58 mg, 0.3 mmol), HOBt (40 mg, 0.3 mmol), and DIPEA (38 mg, 0.3 mmol) in DMF (1 mL) was stirred at room temperature for 30 min under a N_2 atmosphere. The crude compound **11** or **13** (0.24 mmol) was added to the reaction mixture and then stirred overnight. The mixture was concentrated in vacuo followed by addition of acetic acid (0.7 mL). The reaction was heated to 90 °C for 2 h and then diluted with water (10 mL). After extraction with EtOAc (3 × 10 mL), the combined organic phase was washed with brine, dried over Na_2SO_4, filtered, and concentrated in vacuo. The residue was further purified by silica gel column chromatography (CH_2Cl_2/NH_3 7.0 M solution in CH_3OH from 50:1 to 15:1) to afford desired compounds **16** and **17**.

*1-((E)-4-(5-Carbamoyl-2-((E)-2-(1-ethyl-3-methyl-1H-pyrazol-5-yl)vinyl)-7-(3-morpholinopropoxy)-1H-benzo[d]imidazol-1-yl)but-2-en-1-yl)-2-((E)-2-(1-ethyl-3-methyl-1H-pyrazol-5-yl)vinyl)-7-methoxy-1H-benzo[d]imidazole-5-carboxamide (**16**).* White solid;

https://dx.doi.org/10.1021/acs.jmedchem.0c01900
J. Med. Chem. 2021, 64, 1649–1669

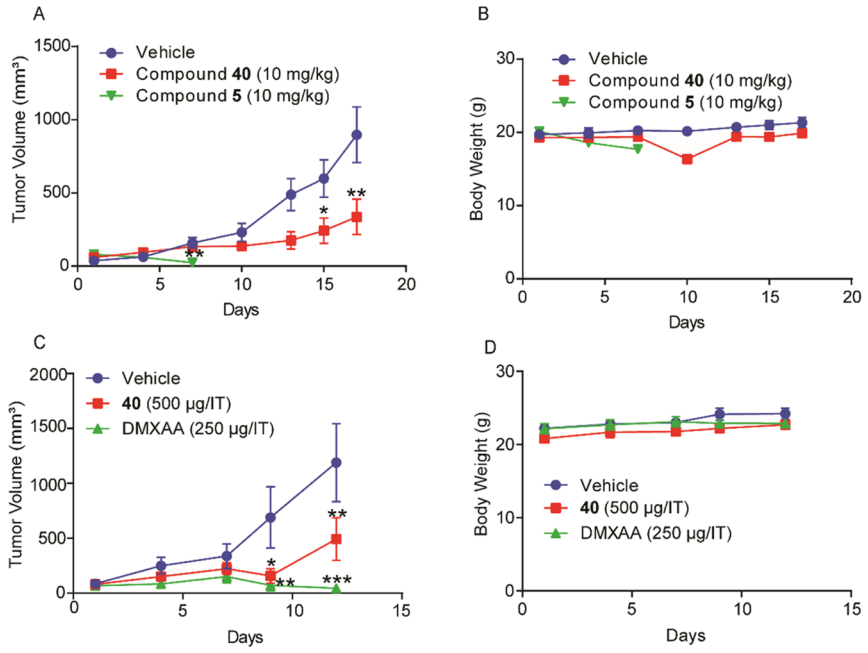

Figure 4. In vivo antitumor effect of compound **40**. (A) Tumor growth in 4T1 orthotopic BALB/c mouse model, compounds **40** and **5** were intravenously injected at days 1, 4, and 7 at a dose of 10 mg/kg. (B) Body weight of 4T1 allograft BALB/c mouse model. (C) Tumor growth in CT26 subcutaneous BALB/c mouse model, compounds **40** and **5** were intratumorally injected at days 1, 4, and 7 at indicated dosages. (D) Body weight of the CT26 allograft mouse model. One-way ANOVA analysis, $*P < 0.05$ and $**P < 0.01$, as compared to the vehicle.

yield: 13%. HPLC purity: 97.5%. ^{1}H NMR (400 MHz, DMSO): δ 7.95 (br, 2H), 7.81 (s, 1H), 7.79 (s, 1H), 7.59 (d, J = 15.3 Hz, 1H), 7.55 (d, J = 14.6 Hz, 1H), 7.26 (br, 2H), 7.24 (s, 1H), 7.17 (s, 1H), 7.09 (d, J = 16.2 Hz, 1H), 7.02 (d, J = 15.6 Hz, 1H), 6.44 (s, 1H), 6.32 (s, 1H), 5.66 (s, 2H), 5.13 (s, 4H), 4.08 (m, 4H), 3.96 (s, 2H), 3.74 (s, 3H), 3.46 (s, 4H), 2.26 (m, 8H), 2.16 (s, 4H), 1.65 (m, 2H), 1.32 (m, 6H). MS (ESI, $[M + H]^+$) m/z, 816.6. HRMS (ESI) calcd for $C_{44}H_{54}N_{11}O_5^+$, 816.4304; found, 816.4292.

*(E)-1-(4-(5-Carbamoyl-2-(2-(1-ethyl-3-methyl-1H-pyrazol-5-yl)-ethyl)-7-(3-morpholinopropoxy)-1H-benzo[d]imidazol-1-yl)but-2-en-1-yl)-2-(2-(1-ethyl-3-methyl-1H-pyrazol-5-yl)ethyl)-7-methoxy-1H-benzo[d]imidazole-5-carboxamide (**17**).* White solid; yield: 16%. HPLC purity: 95.9%. ^{1}H NMR (400 MHz, $CDCl_3$ + CD_3OD): δ 7.78 (s, 2H), 7.12 (s, 1H), 7.08 (s, 1H), 5.79 (s, 1H), 5.73 (s, 1H), 5.58−5.48 (m, 1H), 5.46−5.36 (m, 1H), 4.88 (d, J = 4.6 Hz, 2H), 4.83 (d, J = 5.1 Hz, 2H), 4.08−3.96 (m, 4H), 3.92 (s, 4H), 3.67 (m, 2H), 3.52 (s, 3H), 3.08 (s, 4H), 3.04 (d, J = 4.6 Hz, 4H), 2.98 (m, 4H), 2.70 (br, 2H), 2.23 (s, 3H), 2.21 (s, 3H), 1.79 (m, 2H), 1.41−1.33 (m, 6H). ^{13}C NMR (126 MHz, $CDCl_3$): δ 170.53, 155.88, 155.79, 149.42, 149.26, 146.37, 145.10, 142.99, 142.73, 138.67, 128.51, 128.37, 128.08, 127.55, 126.18, 111.63, 111.12, 104.35, 104.17, 103.58, 65.54, 64.47, 55.28, 54.50, 52.16, 46.03, 45.74, 43.45, 29.58, 27.05, 25.97, 15.29, 10.72. MS (ESI, $[M + H]^+$) m/z, 820.6. HRMS (ESI) calcd for $C_{44}H_{58}N_{11}O_5^+$, 820.4617; found, 820.4602.

General Procedure for Synthesis of Compounds 18 and 22. To a solution of compound **14** or **20** (0.068 mmol) and **15** (32 mg, 0.27 mmol) in MeOH (1 mL) was added 4 N HCl aqueous solution (1 mL). The mixture was stirred at 100 °C for 1 h and then concentrated in vacuo. The residue was further purified by silica gel column chromatography (CH_2Cl_2/NH_3 7.0 M solution in CH_3OH from 50:1 to 20:1) to afford **18** or **22**.

*Methyl (E)-4-(5-Carbamoyl-1-(4-(5-carbamoyl-2-(4-methoxy-4-oxobutanoyl)-7-(3-morpholinopropoxy)-1H-benzo[d]imidazol-1-yl)but-2-en-1-yl)-7-methoxy-1H-benzo[d]imidazol-2-yl)-4-oxobutanoate (**18**).* White solid; yield: 19%. HPLC purity: 95.4%. ^{1}H NMR (400 MHz, DMSO): δ 8.19 (s, 1H), 7.89 (s, 2H), 7.60 (s, 1H), 7.58 (s, 1H), 7.49 (s, 1H), 5.67 (m, 2H), 5.09 (s, 2H), 5.02 (s, 2H), 3.98 (s, 2H), 3.72 (s, 3H), 3.60 (s, 6H), 3.52 (s, 4H), 3.07 (m, 4H), 2.79 (m, 4H), 2.23 (br, 6H), 1.69 (br, 2H). ^{13}C NMR (126 MHz, DMSO): δ 172.76, 172.72, 166.37, 166.29, 158.90, 158.87, 154.65, 147.11, 146.41, 132.98, 132.93, 129.19, 129.12, 127.47, 127.05, 124.59, 124.47, 121.38, 121.26, 112.03, 111.68, 68.14, 66.02, 56.71, 54.70, 53.14, 51.36, 46.61, 46.50, 29.13, 28.01, 25.25. MS (ESI, $[M + H]^+$) m/z, 776.4. HRMS (ESI) calcd for $C_{38}H_{46}N_7O_{11}^+$, 776.3250; found, 776.3267.

*Methyl 4-(5-Carbamoyl-1-((E)-4-((E)-5-carbamoyl-2-((1-ethyl-3-methyl-1H-pyrazole-5-carbonyl)imino)-7-methoxy-2,3-dihydro-1H-benzo[d]imidazol-1-yl)but-2-en-1-yl)-7-(3-morpholinopropoxy)-1H-benzo[d]imidazol-2-yl)-4-oxobutanoate (**22**).* White solid; yield: 20%. HPLC purity: 95.7%. ^{1}H NMR (400 MHz, CD_3OD): δ 7.87 (d, J = 1.9 Hz, 1H), 7.62 (s, 1H), 7.40 (s, 1H), 7.32 (s, 1H), 6.58 (s, 1H), 5.81 (d, J = 16.6 Hz, 1H), 5.71 (d, J = 15.9 Hz, 1H), 5.25 (s, 2H), 4.96 (d, J = 5.2 Hz, 2H), 4.60 (br, 4H), 3.81 (s, 5H), 3.70 (s, 2H), 3.67 (s, 3H), 3.16 (t, J = 6.8 Hz, 2H), 2.85 (t, J = 6.8 Hz, 2H), 2.61 (s, 6H), 2.20 (s, 3H), 1.79 (s, 2H), 1.38−1.32 (m, 3H). MS (ESI, $[M + H]^+$) m/z, 813.4. HRMS (ESI) calcd for $C_{40}H_{49}N_{10}O_9^+$, 813.3678; found, 813.3668.

General Procedure for Synthesis of Compounds 19 and 21. To a solution of compound **14** or **20** (0.068 mmol) and **15** (32 mg, 0.27 mmol) in H_2O (1 mL) was added 4 N HCl aqueous solution (1 mL). The mixture was stirred at 100 °C for 1 h. A white solid was formed and then filtered. The white solid obtained was washed with EtOH followed by vacuum drying to afford compound **19** or **21**.

*(E)-4-(5-Carbamoyl-1-(4-(5-carbamoyl-2-(3-carboxypropanoyl)-7-(3-morpholinopropoxy)-1H-benzo[d]imidazol-1-yl)but-2-en-1-yl)-7-methoxy-1H-benzo[d]imidazol-2-yl)-4-oxobutanoic Acid (**19**).* White solid; yield: 17%. HPLC purity: 95.3%. ^{1}H NMR (400 MHz, DMSO): δ 12.16 (br, 2H), 9.77 (br, 1H), 8.20 (d, J = 3.3 Hz, 2H), 7.98 (d, J = 1.8 Hz, 1H), 7.93 (d, J = 1.9 Hz, 1H), 7.64 (d, J = 1.9 Hz, 1H), 7.61 (d, J = 2.0 Hz, 1H), 7.51 (s, 2H), 5.73 (m, 1H), 5.60 (m, 1H), 5.19−5.07 (m, 2H), 5.00 (dd, J = 4.7, 2.1 Hz, 2H), 4.12 (s, 2H), 4.00 (br, 2H), 3.72 (s, 3H), 3.66 (br, 2H), 3.42 (br, 2H), 3.23 (br, 2H), 3.08 (br, 2H), 3.04 (t, J = 7.0 Hz, 4H), 2.73 (m, 4H), 2.08 (br, 2H). ^{13}C NMR (126 MHz, DMSO): δ 174.31, 174.24, 166.86, 166.78, 159.82, 159.71, 155.34, 155.08, 147.66, 146.59, 133.50, 133.46, 129.68, 129.55, 127.68, 127.17, 125.16, 125.00, 122.10, 121.80, 112.86, 112.16, 67.77, 63.95, 57.31, 54.09, 51.76, 47.46, 47.04, 29.82, 28.59, 28.54, 23.49. MS (ESI, $[M + H]^+$) m/z, 748.3. HRMS (ESI) calcd for $C_{36}H_{42}N_7O_{11}^+$, 748.2937; found, 748.2934.

https://dx.doi.org/10.1021/acs.jmedchem.0c01900
J. Med. Chem. 2021, 64, 1649−1669

*4-(5-Carbamoyl-1-((E)-4-((E)-5-carbamoyl-2-((1-ethyl-3-methyl-1H-pyrazole-5-carbonyl)imino)-7-methoxy-2,3-dihydro-1H-benzo[d]imidazol-1-yl)but-2-en-1-yl)-7-(3-morpholinopropoxy)-1H-benzo[d]imidazol-2-yl)-4-oxobutanoic Acid (**21**).* White solid; yield: 21%. HPLC purity: 99.5%. ^{1}H NMR (400 MHz, DMSO): δ 12.79 (br, 1H), 12.12 (br, 1H), 8.15 (s, 1H), 7.98 (s, 1H), 7.91 (d, J = 1.9 Hz, 1H), 7.66 (d, J = 1.4 Hz, 1H), 7.51 (d, J = 1.9 Hz, 1H), 7.44 (s, 1H), 7.36 (s, 1H), 7.33 (d, J = 1.4 Hz, 1H), 6.52 (s, 1H), 5.75 (d, J = 3.9 Hz, 2H), 5.11 (s, 2H), 4.87 (s, 2H), 4.54 (q, J = 7.1 Hz, 2H), 3.85 (t, J = 6.2 Hz, 2H), 3.78 (s, 3H), 3.44 (t, J = 4.6 Hz, 4H), 3.04 (t, J = 6.9 Hz, 2H), 2.72 (t, J = 6.9 Hz, 2H), 2.14 (d, J = 6.8 Hz, 6H), 2.11 (s, 3H), 1.64−1.52 (m, 2H), 1.29 (t, J = 7.1 Hz, 3H). MS (ESI, $[M + H]^+$) m/z, 799.2. HRMS (ESI) calcd for $C_{39}H_{47}N_{10}O_9^+$, 799.3522; found, 799.3545.

*4-Iodo-2-methoxy-6-nitroaniline (**24**).* To a solution of compound **23** (12.57 g, 74.8 mmol) and Ag_2SO_4 (23.3 g, 74.8 mmol) in EtOH (400 mL) was added I_2 (19.0 g, 74.8 mmol). The mixture was stirred at rt for 1 h and then concentrated in vacuo. The residue was extracted with EtOAc twice, and the combined organic phase was washed with brine, dried over Na_2SO_4, and concentrated in vacuo. The resulting brown solid (15.6 g, 71% yield) was used in the next step without further purification. ^{1}H NMR (400 MHz, $CDCl_3$): δ 8.08 (d, J = 1.8 Hz, 1H), 7.06 (d, J = 1.8 Hz, 1H), 6.47 (br, 2H), 3.91 (s, 3H).

*2-Chloro-5-iodo-1-methoxy-3-nitrobenzene (**25**).* To a solution of compound **24** (6.02 g, 20.5 mmol) in MeOH (120 mL) was added $TsOH·H_2O$ (13.7 g, 72.0 mmol). The mixture was stirred at 0 °C for 10 min followed by adding $NaNO_2$ aqueous solution (2.48 g in 20 mL) slowly. After that, CuCl (5.94 g, 60.0 mmol) was added to the mixture, stirred at 0 °C for 30 min, and then stirred overnight at room temperature. The mixture was concentrated in vacuo and extracted with EtOAc. The combined organic phase was washed with brine, dried over Na_2SO_4, and concentrated in vacuo. The residue was purified by silica gel column chromatography to afford compound **25** (5.65 g) in 88% yield. ^{1}H NMR (400 MHz, $CDCl_3$): δ 7.68 (d, J = 1.7 Hz, 1H), 7.38 (d, J = 1.8 Hz, 1H), 3.96 (s, 3H).

*((4-Chloro-3-methoxy-5-nitrophenyl)ethynyl)trimethylsilane (**26**).* To a solution of compound **25** (2.54 g, 8.1 mmol) in THF (60 mL) were added ethynyltrimethylsilane (3.95 g, 40.3 mmol) and CuI (54 mg, 0.3 mmol), and to DIPEA (4.9 g, 38.2 mmol) was added $PdCl_2(PPh_3)_2$ (282 mg, 0.4 mmol). The mixture was stirred at rt overnight, concentrated in vacuo, and extracted with EtOAc. The combined organic phase was washed with brine, dried over Na_2SO_4, and concentrated in vacuo. The residue was purified by column chromatography to afford compound **26** (1.47 g) in 64% yield. ^{1}H NMR (400 MHz, $CDCl_3$): δ 7.47 (d, J = 1.7 Hz, 1H), 7.14 (d, J = 1.8 Hz, 1H), 3.96 (s, 3H), 0.27 (s, 9H).

*2-Chloro-5-ethynyl-1-methoxy-3-nitrobenzene (**27a**).* To a solution of compound **26** (1.4 g, 4.9 mmol) in MeOH (25 mL) was added K_2CO_3 (0.68 g, 4.9 mmol). The mixture was stirred at rt for 30 min, concentrated in vacuo, and extracted with EtOAc. The combined organic phase was washed with brine, dried over Na_2SO_4, and concentrated in vacuo. The residue was purified by column chromatography to afford **27a** (0.96 g) in 93% yield. ^{1}H NMR (400 MHz, $CDCl_3$): δ 7.49 (s, 1H), 7.18 (s, 1H), 3.97 (s, 3H), 3.23 (s, 1H).

General Procedure for Synthesis of Compounds 28a and 28d. To a solution of chlorides **27a**−**27d** (1 equiv) and *tert*-butyl (*E*)-(4-aminobut-2-en-1-yl)carbamate (2 equiv) in EtOH was added DIPEA (2 equiv). The mixture was stirred at 120 °C in a sealed tube for 2 days and then concentrated in vacuo. The residue was further purified by column chromatography to afford compounds **28a** and **28d** in 26 and 52% yields, respectively.

*tert-Butyl (E)-(4-((4-Ethynyl-2-methoxy-6-nitrophenyl)amino)-but-2-en-1-yl)carbamate (**28a**).* Yield: 26%. ^{1}H NMR (400 MHz, $CDCl_3$): δ 7.91 (d, J = 1.8 Hz, 1H), 7.82 (br, 1H), 6.94 (s, 1H), 5.68 (d, J = 5.3 Hz, 2H), 4.58 (br, 1H), 4.18 (t, J = 5.2 Hz, 2H), 3.84 (s, 3H), 3.72 (s, 2H), 3.01 (s, 1H), 1.44 (s, 9H).

*Methyl (E)-4-((4-((tert-Butoxycarbonyl)amino)but-2-en-1-yl)-amino)-3-methoxy-5-nitrobenzoate (**28d**).* Yield: 42%. ^{1}H NMR (400 MHz, $CDCl_3$): δ 8.47 (d, J = 1.9 Hz, 1H), 8.11 (br, 1H), 7.48 (d, J = 2.0 Hz, 1H), 5.70 (m, 2H), 4.59 (br, 1H), 4.31−4.22 (m, 2H), 3.90 (s, 3H), 3.89 (s, 3H), 3.73 (s, 2H), 1.44 (s, 9H).

*tert-Butyl (E)-(4-((2-Methoxy-4-(1-(2-(2-methoxyethoxy)ethyl)-1H-1,2,3-triazol-4-yl)-6-nitrophenyl)amino)but-2-en-1-yl)-carbamate (**29a**).* To a solution of 1-azido-2-(2-methoxyethoxy)-ethane (65 mg, 0.45 mmol) in a mixture of *t*-BuOH and H_2O (2:1, 3 mL) were added sodium ascorbate (30 mg, 0.15 mmol), $CuSO_4·5H_2O$ (4 mg, 0.015 mmol), and **28a** (108 mg, 0.3 mmol). The reaction mixture was stirred at rt for 1 h; then, saturated sodium bicarbonate solution was added, and the mixture was extracted with EtOAc. The combined organic phase was washed with brine, dried over Na_2SO_4, and concentrated in vacuo. The residue was subjected to column chromatography to afford the title compound in 52% yield. ^{1}H NMR (400 MHz, CD_3OD): δ 8.39 (s, 1H), 8.08 (d, J = 1.9 Hz, 1H), 7.55 (d, J = 2.0 Hz, 1H), 5.76−5.56 (m, 2H), 4.62 (t, J = 5.0 Hz, 2H), 4.15 (d, J = 4.9 Hz, 2H), 3.96 (s, 3H), 3.92 (t, J = 5.0 Hz, 2H), 3.67−3.61 (m, 2H), 3.60 (s, 2H), 3.56−3.49 (m, 2H), 3.33 (d, J = 2.6 Hz, 2H), 1.40 (s, 9H).

General Procedure for Synthesis of Compounds 29b and 32c. To a solution of benzonitrile **28b** or **32b** (1 equiv) in MeOH was added NaOMe (0.5 equiv). The mixture was stirred at rt for 3 h, and then 2,2-dimethoxyethan-1-amine (1 equiv) and AcOH (2 equiv) were added. The mixture was stirred at 50 °C for another 2 h, and then a solution of 6 N HCl solution was added to adjust pH = 1. The mixture was stirred at 70 °C for 18 h, concentrated in vacuo, and then diluted with water. A solution of 2 M Na_2CO_3 aqueous solution was added to adjust the pH value of the mixture to 10. The mixture was filtered, and the solid was dried to afford compound **29b** or **32c** in 56 and 68% yields, respectively.

*tert-Butyl (E)-(4-((4-(1H-Imidazol-2-yl)-2-methoxy-6-nitrophenyl)amino)but-2-en-1-yl)carbamate (**29b**).* ^{1}H NMR (400 MHz, DMSO): δ 12.63 (br, 1H), 8.19 (s, 1H), 7.69 (s, 1H), 7.63 (t, J = 6.3 Hz, 1H), 7.13 (s, 2H), 6.96 (s, 1H), 5.56 (s, 2H), 4.09 (s, 2H), 3.91 (s, 3H), 3.49 (s, 2H), 1.35 (s, 9H).

*4-(3-(2-Chloro-5-(1H-imidazol-2-yl)-3-nitrophenoxy)propyl)-morpholine (**32c**).* ^{1}H NMR (600 MHz, DMSO): δ 12.96 (br, 1H), 8.10 (d, J = 1.8 Hz, 1H), 7.99 (s, 1H), 7.38 (br, 1H), 7.12 (br, 1H), 4.30 (s, 2H), 3.59 (br, 4H), 2.39 (m, 6H), 2.01 (m, 2H).

General Procedure for Synthesis of Compounds 29c, 29d, and 32d. A solution of benzamide **28c** or **32a** (1 equiv) in DMF-DMA was stirred at 100 °C for 1 h, cooled to rt, and then concentrated in vacuo. The residue was diluted in EtOH, hydrazine acetate (2 equiv) was added, and the resulting mixture was heated to 50 °C. After 30 min, the mixture was concentrated in vacuo and the residue was diluted in H_2O. After filtration, the obtained solid was washed with EtOH and dried. Compounds **29c**, **29d**, and **32d** were obtained in 49−72% yields.

*tert-Butyl (E)-(4-((2-Methoxy-6-nitro-4-(1H-1,2,4-triazol-5-yl)-phenyl)amino)but-2-en-1-yl)carbamate (**29c**).* ^{1}H NMR (400 MHz, DMSO): δ 14.18 (br, 1H), 8.44 (br, 1H), 8.24 (d, J = 1.9 Hz, 1H), 7.72 (s, 1H), 7.65 (d, J = 1.9 Hz, 1H), 6.96 (t, J = 6.0 Hz, 1H), 5.63−5.46 (m, 2H), 4.11 (d, J = 6.0 Hz, 2H), 3.92 (s, 3H), 3.48 (d, J = 5.5 Hz, 2H), 1.35 (s, 9H).

*tert-Butyl (E)-(4-((2-Methoxy-4-(3-methyl-1H-1,2,4-triazol-5-yl)-6-nitrophenyl)amino)but-2-en-1-yl)carbamate (**29d**).* ^{1}H NMR (400 MHz, CD_3OD): δ 8.33 (d, J = 1.9 Hz, 1H), 7.67 (d, J = 1.9 Hz, 1H), 5.76−5.53 (m, 2H), 4.21 (s, 2H), 3.98 (s, 3H), 3.62 (d, J = 2.1 Hz, 2H), 2.49 (s, 3H), 1.42 (s, 9H).

*4-(3-(2-Chloro-3-nitro-5-(1H-1,2,4-triazol-5-yl)phenoxy)propyl)-morpholine (**32d**).* ^{1}H NMR (400 MHz, CD_3OD): δ 8.53 (s, 1H), 8.05 (d, J = 1.8 Hz, 1H), 7.98 (d, J = 1.9 Hz, 1H), 4.32 (t, J = 6.1 Hz, 2H), 3.70 (t, J = 4.7 Hz, 4H), 2.63 (t, J = 7.4 Hz, 2H), 2.53 (s, 4H), 2.10 (m, 2H).

*tert-Butyl (E)-(4-((4-((2-Hydroxyethyl)carbamoyl)-2-methoxy-6-nitrophenyl)amino)but-2-en-1-yl)carbamate (**30**).* To a solution of **28d** (645 mg, 1.63 mmol) in MeOH (10 mL) was added 2-aminoethan-1-ol (0.6 mL, 6.5 mmol). The mixture was stirred at 70 °C for 14 h and then concentrated in vacuo. The residue was purified by column chromatography to afford compound **30** in 85% yield. ^{1}H NMR (400 MHz, $CDCl_3$): δ 8.07 (d, J = 2.0 Hz, 2H), 7.41 (d, J = 2.0

https://dx.doi.org/10.1021/acs.jmedchem.0c01900
J. Med. Chem. 2021, 64, 1649−1669

Hz, 1H), 7.13 (s, 1H), 5.67 (m, 2H), 4.76 (s, 1H), 4.22 (t, J = 5.0 Hz, 2H), 3.84 (s, 3H), 3.82 (d, J = 4.9 Hz, 2H), 3.71 (d, J = 5.4 Hz, 2H), 3.59 (q, J = 5.2 Hz, 2H), 3.49 (s, 1H), 1.42 (s, 9H).

*tert-Butyl (E)-(4-((4-(4,5-Dihydrooxazol-2-yl)-2-methoxy-6-nitrophenyl)amino)but-2-en-1-yl)carbamate (**29e**).* To a solution of **30** (170 mg, 0.4 mmol) in DCM (3 mL) was added $SOCl_2$ (66 μL, 0.9 mmol) at 0 °C. The mixture was stirred at 0 °C for 0.5 h and then concentrated in vacuo. The residue was added ice water, and the mixture was alkalized by saturated sodium bicarbonate solution to pH = 9. After concentration in vacuo, the residue was diluted with EtOAc and water. The organic phase was washed with brine, dried over Na_2SO_4, and concentrated in vacuo. The residue was subjected to column chromatography to afford compound **29e** in 45% yield over two steps. ^{1}H NMR (400 MHz, $CDCl_3$): δ 8.28 (d, J = 1.9 Hz, 1H), 8.03 (t, J = 5.5 Hz, 1H), 7.47 (d, J = 1.9 Hz, 1H), 5.69 (m, 2H), 4.58 (br, 1H), 4.43 (t, J = 9.5 Hz, 2H), 4.29–4.18 (m, 2H), 4.04 (t, J = 9.4 Hz, 2H), 3.88 (s, 3H), 3.73 (s, 2H), 1.44 (s, 9H).

General Procedure for Synthesis of Compounds 33a–33l and 47. To a solution of **29a–29e** in MeOH (1 mL) was added 4 N HCl aqueous solution (1 mL). The mixture was stirred at rt for 1 h and then concentrated in vacuo. The obtained intermediates were used without further purification. To a solution of the crude hydrochloride salts of amines (1 equiv) and corresponding aryl chlorides **32a–32d** (1.2 equiv) in *i*-PrOH was added DIPEA (3 equiv). The mixture was stirred at 120 °C in a sealed tube for 2 days and then concentrated in vacuo. The residue was purified by column chromatography to afford the key intermediates **33a–33l** or **47** in 31–50% overall yields.

*(E)-4-((4-((4-Cyano-2-(3-morpholinopropoxy)-6-nitrophenyl)amino)but-2-en-1-yl)amino)-3-methoxy-5-nitrobenzonitrile (**33a**).* Crimson solid; yield: 38%. ^{1}H NMR (400 MHz, DMSO): δ 7.93 (m, 2H), 7.35 (d, J = 1.8 Hz, 2H), 5.49 (d, J = 3.1 Hz, 2H), 4.07 (m, 2H), 4.04–3.97 (m, 4H), 3.80 (s, 3H), 3.55 (t, J = 4.6 Hz, 4H), 2.35 (m, 6H), 1.86 (m, 2H).

*(E)-N^1-(2-Methoxy-6-nitro-4-(1H-1,2,4-triazol-5-yl)phenyl)-N^4-(2-(3-morpholinopropoxy)-6-nitro-4-(1H-1,2,4-triazol-5-yl)phenyl)-but-2-ene-1,4-diamine (**33b**).* Crimson solid; yield: 42%. ^{1}H NMR (400 MHz, DMSO): δ 8.36 (s, 2H), 8.19 (d, J = 6.4 Hz, 2H), 7.58 (s, 2H), 5.63 (m, 2H), 4.13 (s, 2H), 4.08 (s, 2H), 4.03 (t, J = 6.2 Hz, 2H), 3.83 (s, 3H), 3.59–3.51 (m, 4H), 2.38 (t, J = 7.0 Hz, 2H), 2.32 (s, 4H), 1.94–1.83 (m, 1H).

*(E)-N^1-(4-(1H-Imidazol-2-yl)-2-(3-morpholinopropoxy)-6-nitrophenyl)-N^4-(4-(1H-imidazol-2-yl)-2-methoxy-6-nitrophenyl)but-2-ene-1,4-diamine (**33c**).* Crimson solid; yield: 48%. ^{1}H NMR (400 MHz, $CDCl_3$): δ 7.91 (m, 2H), 7.59 (t, J = 7.1 Hz, 2H), 7.31 (dd, J = 4.5, 2.0 Hz, 2H), 7.27 (m, 2H), 5.36 (s, 2H), 4.04 (s, 4H), 3.69 (t, J = 4.7 Hz, 4H), 3.63 (t, J = 6.5 Hz, 2H), 3.49 (s, 3H), 2.40 (s, 4H), 2.35 (t, J = 7.3 Hz, 2H), 1.91–1.77 (m, 2H).

*(E)-4-((4-((2-Methoxy-6-nitro-4-(4H-1,2,4-triazol-3-yl)phenyl)amino)but-2-en-1-yl)amino)-3-(3-morpholinopropoxy)-5-nitrobenzonitrile (**33d**).* Crimson solid; yield: 45%. ^{1}H NMR (400 MHz, DMSO): δ 8.15 (dd, J = 5.3, 1.9 Hz, 2H), 8.08 (s, 1H), 7.76 (t, J = 6.3 Hz, 1H), 7.64 (d, J = 1.9 Hz, 1H), 7.56 (t, J = 6.3 Hz, 1H), 7.51 (s, 1H), 7.33 (s, 1H), 7.12 (s, 2H), 5.71–5.53 (m, 2H), 4.12 (t, J = 5.0 Hz, 2H), 4.06 (t, J = 5.1 Hz, 2H), 4.01 (t, J = 6.3 Hz, 2H), 3.84 (s, 3H), 3.54 (t, J = 4.6 Hz, 4H), 2.40 (t, J = 7.1 Hz, 2H), 2.34 (s, 4H), 1.88 (t, J = 6.8 Hz, 2H).

*(E)-4-((4-((4-(4,5-Dihydrooxazol-2-yl)-2-methoxy-6-nitrophenyl)amino)but-2-en-1-yl)amino)-3-(3-morpholinopropoxy)-5-nitrobenzamide (**33f**).* Crimson solid; yield: 50%. ^{1}H NMR (400 MHz, $CDCl_3$): δ 8.22 (d, J = 1.9 Hz, 1H), 8.06 (d, J = 1.9 Hz, 1H), 8.00 (s, 2H), 7.49 (s, 1H), 7.35 (s, 1H), 5.69–5.58 (m, 2H), 4.48 (t, J = 9.5 Hz, 2H), 4.23 (dd, J = 11.9, 5.9 Hz, 4H), 4.07 (dd, J = 12.2, 6.4 Hz, 4H), 3.80 (s, 3H), 3.72 (t, J = 4.6 Hz, 4H), 2.48 (dd, J = 14.6, 7.4 Hz, 6H), 2.01 (t, J = 6.7 Hz, 3H).

*(E)-4-((4-((2-Methoxy-6-nitro-4-(1H-1,2,4-triazol-5-yl)phenyl)amino)but-2-en-1-yl)amino)-3-(3-morpholinopropoxy)-5-nitrobenzamide (**33g**).* Crimson solid; yield: 39%. ^{1}H NMR (400 MHz, DMSO): δ 8.42 (s, 1H), 8.21 (d, J = 1.9 Hz, 1H), 8.17 (d, J = 1.9 Hz, 1H), 8.04 (s, 1H), 7.78 (t, J = 6.3 Hz, 1H), 7.68 (t, J = 6.2 Hz, 1H), 7.62 (d, J = 1.9 Hz, 1H), 7.51 (d, J = 2.0 Hz, 1H), 7.33 (s, 1H), 5.70–5.51 (m, 2H), 4.13 (d, J = 5.7 Hz, 2H), 4.07 (d, J = 6.0 Hz, 2H), 4.02 (dd, J = 8.2, 4.4 Hz, 2H), 3.86 (s, 3H), 3.55 (m, 4H), 2.36 (m, 2H), 2.31 (s, 4H), 1.93–1.81 (m, 2H).

*(E)-4-((4-((2-Methoxy-4-(3-methyl-1H-1,2,4-triazol-5-yl)-6-nitrophenyl)amino)but-2-en-1-yl)amino)-3-(3-morpholinopropoxy)-5-nitrobenzamide (**33h**).* Crimson solid; yield: 37%. ^{1}H NMR (400 MHz, CD_3OD): δ 6.98 (d, J = 1.8 Hz, 1H), 6.95 (d, J = 1.9 Hz, 1H), 6.92 (d, J = 1.9 Hz, 1H), 6.86 (d, J = 2.0 Hz, 1H), 5.73 (m, 2H), 3.98 (t, J = 6.1 Hz, 2H), 3.80 (s, 3H), 3.66 (t, J = 4.7 Hz, 4H), 3.60–3.55 (m, 2H), 3.55–3.49 (m, 2H), 2.54–2.46 (m, 2H), 2.45 (s, 2H), 2.44 (s, 3H), 2.01–1.87 (m, 2H).

*(E)-4-((4-((2-Methoxy-4-(1-(2-(2-methoxyethoxy)ethyl)-1H-1,2,3-triazol-4-yl)-6-nitrophenyl)amino)but-2-en-1-yl)amino)-3-(3-morpholinopropoxy)-5-nitrobenzamide (**33i**).* Crimson solid; yield: 50%. ^{1}H NMR (400 MHz, CD_3OD): δ 8.35 (s, 1H), 7.93 (s, 1H), 7.82 (s, 1H), 7.39 (s, 1H), 5.63 (s, 2H), 4.64 (t, J = 5.1 Hz, 2H), 4.29 (t, J = 6.0 Hz, 2H), 3.99–3.92 (m, 2H), 3.84 (s, 3H), 3.75–3.64 (m, 13H), 3.57–3.49 (m, 2H), 2.64 (m, 2H), 2.53 (m, 4H), 2.13–2.05 (m, 2H).

*(E)-3-Methoxy-4-((4-((2-(3-morpholinopropoxy)-6-nitro-4-(4H-1,2,4-triazol-3-yl)phenyl)amino)but-2-en-1-yl)amino)-5-nitrobenzamide (**33k**).* Crimson solid; yield: 43%. ^{1}H NMR (400 MHz, CD_3OD): δ 8.33 (s, 1H), 8.25 (s, 1H), 8.18 (s, 1H), 7.53 (s, 1H), 7.40 (s, 1H), 5.69 (s, 2H), 4.18–4.10 (m, 4H), 4.07–3.96, (m, 4H), 3.91 (s, 2H), 3.81 (s, 3H), 3.70 (s, 4H), 2.50 (m, 6H), 2.01 (m, 2H).

*(E)-3-(3-((tert-Butyldimethylsilyl)oxy)propoxy)-4-((4-((2-methoxy-6-nitro-4-(1H-1,2,4-triazol-5-yl)phenyl)amino)but-2-en-1-yl)-amino)-5-nitrobenzamide (**47**).* Crimson solid; yield: 39%. ^{1}H NMR (400 MHz, CD_3OD): δ 8.21 (s, 1H), 7.02 (d, J = 1.8 Hz, 1H), 6.99 (d, J = 1.9 Hz, 1H), 6.92 (d, J = 1.9 Hz, 1H), 6.88 (d, J = 2.0 Hz, 1H), 5.74 (t, J = 3.1 Hz, 2H), 5.74 (t, J = 3.1 Hz, 2H), 4.05 (t, J = 6.0 Hz, 2H), 3.82 (s, 3H), 3.79 (t, J = 6.1 Hz, 2H), 3.56 (d, J = 3.4 Hz, 2H), 3.55–3.49 (m, 2H), 1.95 (m, J = 6.1 Hz, 2H), 0.86 (s, 9H), 0.01 (s, 6H).

Reduction of **33a–33l** and subsequent generation of the imidazole ring using 1-ethyl-3-methyl-1*H*-pyrazole-5-carbonyl isothiocyanate were conducted by following literature procedures.[24] The final compounds were purified by silica gel column chromatography (CH_2Cl_2/NH_3 7.0 M solution in CH_3OH from 50:1 to 10:1).

*N-((E)-5-Cyano-1-((E)-4-((E)-5-cyano-2-((1-ethyl-3-methyl-1H-pyrazole-5-carbonyl)imino)-7-(3-morpholinopropoxy)-2,3-dihydro-1H-benzo[d]imidazol-1-yl)but-2-en-1-yl)-7-methoxy-1,3-dihydro-2H-benzo[d]imidazol-2-ylidene)-1-ethyl-3-methyl-1H-pyrazole-5-carboxamide (**34**).* White solid; yield: 32%. HPLC purity: 100%. ^{1}H NMR (400 MHz, $CDCl_3$): δ 7.24 (s, 1H), 6.91 (s, 1H), 6.88 (s, 1H), 6.57 (s, 1H), 6.55 (s, 1H), 5.81 (s, 2H), 4.94 (br, 4H), 4.65–4.44 (m, 4H), 3.96 (br, 2H), 3.73 (s, 3H), 3.64 (br, 4H), 2.31 (br, 6H), 2.20 (s, 3H), 2.20 (s, 3H), 1.78 (br, 2H), 1.36 (m, 6H). ^{13}C NMR (126 MHz, $CDCl_3$): δ 169.15, 169.13, 168.92, 168.89, 153.54, 153.37, 146.58, 146.14, 145.51, 139.68, 129.94, 129.81, 128.42, 121.54, 121.39, 118.69, 110.15, 109.79, 109.11, 109.06, 108.90, 106.78, 77.42, 77.16, 76.91, 67.63, 66.75, 56.19, 55.12, 53.59, 46.58, 45.21, 25.90, 16.18, 16.18, 13.25, 13.23. MS (ESI, $[M + H]^+$) m/z, 814.3. HRMS (ESI) calcd for $C_{42}H_{48}N_{13}O_5^+$, 814.3896; found, 814.3899.

*1-Ethyl-N-((E)-1-((E)-4-((E)-2-((1-ethyl-3-methyl-1H-pyrazole-5-carbonyl)imino)-7-(3-morpholinopropoxy)-5-(1H-1,2,4-triazol-5-yl)-2,3-dihydro-1H-benzo[d]imidazol-1-yl)but-2-en-1-yl)-7-methoxy-5-(1H-1,2,4-triazol-5-yl)-1,3-dihydro-2H-benzo[d]imidazol-2-ylidene)-3-methyl-1H-pyrazole-5-carboxamide (**35**).* White solid; yield: 37%. HPLC purity: 100%. ^{1}H NMR (500 MHz, CD_3OD): δ 8.27 (s, 1H), 8.25 (s, 1H), 7.51 (s, 1H), 7.48 (s, 1H), 7.11 (s, 1H), 7.05 (s, 1H), 6.49 (s, 1H), 6.39 (s, 1H), 5.62 (m, 2H), 4.72 (m, 4H), 4.47 (m, 4H), 3.70 (br, 2H), 3.53 (br, 7H), 2.28 (br, 6H), 2.13 (s, 3H), 2.07 (s, 3H), 1.61 (s, 2H), 1.28 (t, J = 7.2 Hz, 3H), 1.23 (t, J = 7.3 Hz, 3H). ^{13}C NMR (126 MHz, CD_3OD): δ 168.90, 160.24, 153.52, 153.48, 147.46, 147.40, 147.13, 146.36, 141.70, 141.55, 131.70, 129.60, 129.15, 126.62, 119.85, 110.66, 105.23, 104.70, 103.80, 67.91, 67.31, 56.48, 56.09, 54.39, 47.24, 45.71, 26.79, 16.66, 16.64, 13.14. MS (ESI, $[M + H]^+$) m/z, 898.4. HRMS (ESI) calcd for $C_{44}H_{52}N_{17}O_5^+$, 898.4332; found, 898.4335.

https://dx.doi.org/10.1021/acs.jmedchem.0c01900
J. Med. Chem. 2021, 64, 1649–1669

*1-Ethyl-N-((E)-1-((E)-4-((E)-2-((1-ethyl-3-methyl-1H-pyrazole-5-carbonyl)imino)-5-(1H-imidazol-2-yl)-7-(3-morpholinopropoxy)-2,3-dihydro-1H-benzo[d]imidazol-1-yl)but-2-en-1-yl)-5-(1H-imidazol-2-yl)-7-methoxy-1,3-dihydro-2H-benzo[d]imidazol-2-ylidene)-3-methyl-1H-pyrazole-5-carboxamide (**36**).* White solid; yield: 35%. HPLC purity: 97.4%. ^{1}H NMR (400 MHz, $CDCl_3$): δ 7.28 (br, 2H), 7.07 (br, 4H), 6.99 (d, J = 1.4 Hz, 1H), 6.95 (d, J = 1.3 Hz, 1H), 6.63 (s, 1H), 6.60 (s, 1H), 5.70−5.67 (m, 2H), 4.85 (m, 4H), 4.59 (m, 4H), 3.55 (m, 4H), 3.49 (m, 2H), 3.31 (s, 3H), 2.24 (br, 4H), 2.21 (s, 3H), 2.19 (s, 3H), 2.17 (m, 2H), 1.51 (m, 2H), 1.39 (m, 6H). ^{13}C NMR (151 MHz, CD_3OD): δ 168.85, 168.64, 153.02, 152.90, 146.60, 146.58, 146.43, 146.40, 146.04, 145.38, 140.21, 140.10, 130.08, 129.77, 128.84, 128.72, 126.71, 123.78, 117.93, 117.83, 109.93, 104.00, 103.42, 101.42, 101.28, 66.71, 66.65, 55.44, 55.03, 53.50, 46.53, 44.71, 44.67, 25.94, 16.27, 13.25, 13.23. MS (ESI, $[M + H]^+$) m/z, 896.5. HRMS (ESI) calcd for $C_{46}H_{54}N_{15}O_5^+$, 896.4427; found, 896.4438.

*N-((E)-5-Cyano-1-((E)-4-((E)-2-((1-ethyl-3-methyl-1H-pyrazole-5-carbonyl)imino)-7-methoxy-5-(1H-1,2,4-triazol-5-yl)-2,3-dihydro-1H-benzo[d]imidazol-1-yl)but-2-en-1-yl)-7-(3-morpholinopropoxy)-1,3-dihydro-2H-benzo[d]imidazol-2-ylidene)-1-ethyl-3-methyl-1H-pyrazole-5-carboxamide (**37**).* White solid; yield: 29%. HPLC purity: 95.4%. ^{1}H NMR (400 MHz, CD_3OD): δ 8.38 (s, 1H), 7.51 (s, 1H), 7.14 (s, 1H), 7.08 (s, 1H), 6.64 (s, 1H), 6.45 (s, 1H), 6.34 (s, 1H), 5.66−5.47 (m, 2H), 4.77−4.60 (m, 4H), 4.55−4.32 (m, 4H), 3.66 (br, 2H), 3.58 (s, 3H), 3.50 (m, 4H), 2.31−2.15 (m, 6H), 2.10 (s, 6H), 1.55 (m, 2H), 1.30−1.15 (m, 6H). ^{13}C NMR (151 MHz, CD_3OD): δ 167.37, 152.58, 152.16, 146.12, 146.01, 145.77, 145.03, 140.09, 139.72, 130.34, 128.14, 127.77, 125.59, 120.98, 118.40, 118.32, 109.46, 109.25, 108.86, 105.90, 103.32, 102.43, 67.15, 66.04, 54.97, 54.81, 53.04, 45.88, 44.49, 44.40, 25.37, 15.28, 15.23, 11.83, 11.77. MS (ESI, $[M + H]^+$) m/z, 856.4. HRMS (ESI) calcd for $C_{43}H_{50}N_{15}O_5^+$, 856.4114; found, 856.4097.

*(E)-2-((1-Ethyl-3-methyl-1H-pyrazole-5-carbonyl)imino)-1-((E)-4-((E)-2-((1-ethyl-3-methyl-1H-pyrazole-5-carbonyl)imino)-5-(1H-imidazol-2-yl)-7-methoxy-2,3-dihydro-1H-benzo[d]imidazol-1-yl)-but-2-en-1-yl)-7-(3-morpholinopropoxy)-2,3-dihydro-1H-benzo[d]-imidazole-5-carboxamide (**38**).* White solid; yield: 34%. HPLC purity: 98.1%. ^{1}H NMR (400 MHz, CD_3OD): δ 7.41 (d, J = 1.1 Hz, 1H), 7.37 (d, J = 1.2 Hz, 1H), 7.10 (s, 2H), 7.03 (s, 1H), 7.01 (s, 1H), 6.48 (s, 1H), 6.40 (s, 1H), 5.63 (m, 2H), 4.77 (s, 2H), 4.70 (s, 2H), 4.54−4.38 (m, 4H), 3.68 (t, J = 5.9 Hz, 2H), 3.56−3.47 (m, 7H), 2.24−2.16 (m, 6H), 2.11 (s, 3H), 2.10 (s, 3H), 1.56 (m, 2H), 1.25 (m, 6H). ^{13}C NMR (126 MHz, CD_3OD): δ 171.18, 168.98, 168.81, 153.90, 153.43, 147.53, 147.45, 147.40, 147.30, 146.04, 141.54, 141.49, 131.82, 131.38, 130.63, 129.52, 129.26, 127.63, 121.45, 119.09, 110.70, 110.65, 106.57, 105.70, 103.97, 102.55, 68.15, 67.53, 56.54, 56.13, 54.52, 47.23, 45.77, 26.97, 16.65, 13.19, 13.14. MS (ESI, $[M + H]^+$) m/z, 873.4. HRMS (ESI) calcd for $C_{44}H_{53}N_{14}O_6^+$, 873.4267; found, 873.4267.

*(E)-1-((E)-4-((E)-5-(4,5-Dihydrooxazol-2-yl)-2-((1-ethyl-3-methyl-1H-pyrazole-5-carbonyl)imino)-7-methoxy-2,3-dihydro-1H-benzo-[d]imidazol-1-yl)but-2-en-1-yl)-2-((1-ethyl-3-methyl-1H-pyrazole-5-carbonyl)imino)-7-(3-morpholinopropoxy)-2,3-dihydro-1H-benzo[d]imidazole-5-carboxamide (**39**).* White solid; yield: 42%. HPLC purity: 100%. ^{1}H NMR (400 MHz, CD_3OD): δ 7.47 (s, 1H), 7.46 (s, 1H), 7.07 (s, 2H), 6.56 (s, 1H), 6.50 (s, 1H), 5.78−5.64 (m, 2H), 4.84 (m, 4H), 4.60−4.45 (m, 6H), 4.01 (t, J = 9.5 Hz, 2H), 3.79 (t, J = 6.1 Hz, 2H), 3.57 (s, 3H), 3.55 (m, 4H), 2.32−2.23 (m, 6H), 2.18 (s, 3H), 2.16 (s, 3H), 1.71−1.62 (m, 2H), 1.36−1.28 (m, 6H). ^{13}C NMR (126 MHz, CD_3OD): δ 171.17, 169.02, 166.54, 154.00, 147.66, 146.93, 146.21, 141.57, 131.57, 130.84, 129.57, 129.48, 124.32, 121.68, 110.77, 106.79, 106.40, 69.30, 68.26, 67.60, 56.66, 56.24, 55.17, 54.61, 47.31, 45.96, 27.07, 16.66, 13.18. MS (ESI, $[M + H]^+$) m/z, 876.3. HRMS (ESI) calcd for $C_{44}H_{54}N_{13}O_7^+$, 876.4264; found, 876.4262.

*(E)-2-((1-Ethyl-3-methyl-1H-pyrazole-5-carbonyl)imino)-1-((E)-4-((E)-2-((1-ethyl-3-methyl-1H-pyrazole-5-carbonyl)imino)-7-methoxy-5-(1H-1,2,4-triazol-5-yl)-2,3-dihydro-1H-benzo[d]imidazol-1-yl)but-2-en-1-yl)-7-(3-morpholinopropoxy)-2,3-dihydro-1H-benzo-[d]imidazole-5-carboxamide (**40**).* White solid; yield: 39%. HPLC purity: 99.7%. ^{1}H NMR (400 MHz, CD_3OD): δ 8.41 (s, 1H), 7.69 (d, J = 1.3 Hz, 1H), 7.52 (s, 1H), 7.36 (s, 1H), 7.16 (d, J = 1.4 Hz, 1H), 6.60 (s, 1H), 6.52 (s, 1H), 5.80 (s, 2H), 4.97 (s, 2H), 4.94 (s, 2H), 4.56 (m, 4H), 3.87 (t, J = 6.1 Hz, 2H), 3.70 (s, 3H), 3.56 (t, J = 4.6 Hz, 3H), 2.31 (m, 6H), 2.19 (s, 3H), 2.18 (s, 3H), 1.68 (m, 2H), 1.33 (m, 6H). ^{13}C NMR (126 MHz, CD_3OD): δ 169.74, 167.65, 167.45, 159.13, 152.52, 152.14, 146.09, 146.05, 145.84, 144.67, 140.20, 140.13, 130.39, 129.96, 129.27, 128.11, 127.93, 125.47, 120.07, 118.54, 109.33, 105.21, 104.35, 103.42, 102.52, 66.79, 66.18, 55.17, 54.78, 53.16, 45.86, 44.41, 43.66, 25.61, 15.27, 11.81, 11.78. MS (ESI, $[M + H]^+$) m/z, 874.4. HRMS (ESI) calcd for $C_{43}H_{52}N_{15}O_6^+$, 874.4220; found, 874.4222.

*(E)-2-((1-Ethyl-3-methyl-1H-pyrazole-5-carbonyl)imino)-1-((E)-4-((E)-2-((1-ethyl-3-methyl-1H-pyrazole-5-carbonyl)imino)-7-methoxy-5-(3-methyl-1H-1,2,4-triazol-5-yl)-2,3-dihydro-1H-benzo[d]-imidazol-1-yl)but-2-en-1-yl)-7-(3-morpholinopropoxy)-2,3-dihydro-1H-benzo[d]imidazole-5-carboxamide (**41**).* White solid; yield: 31%. HPLC purity: 100%. ^{1}H NMR (400 MHz, CD_3OD): δ 7.60 (d, J = 1.3 Hz, 1H), 7.49 (d, J = 1.3 Hz, 1H), 7.27 (d, J = 1.4 Hz, 1H), 7.12 (d, J = 1.5 Hz, 1H), 6.58 (s, 1H), 6.49 (s, 1H), 5.83−5.68 (m, 2H), 4.92 (d, J = 3.7 Hz, 2H), 4.87 (s, 2H), 4.63−4.51 (m, 4H), 3.83 (t, J = 6.1 Hz, 2H), 3.66 (s, 3H), 3.54 (t, J = 4.6 Hz, 4H), 2.48 (s, 3H), 2.27 (m, 6H), 2.18 (s, 3H), 2.17 (s, 3H), 1.65 (m, 2H), 1.34 (t, J = 7.2 Hz, 3H), 1.30 (t, J = 7.1 Hz, 3H). ^{13}C NMR (126 MHz, CD_3OD): δ 171.23, 168.95, 153.68, 147.63, 147.58, 147.39, 146.24, 141.69, 131.93, 130.82, 129.50, 129.43, 119.99, 110.68, 106.76, 104.86, 103.84, 68.28, 67.60, 56.63, 56.25, 54.59, 49.00, 47.28, 45.89, 27.06, 16.66, 13.19, 13.15. MS (ESI, $[M + H]^+$) m/z, 888.4. HRMS (ESI) calcd for $C_{44}H_{54}N_{15}O_6^+$, 888.4376; found, 888.4395.

*(E)-2-((1-Ethyl-3-methyl-1H-pyrazole-5-carbonyl)imino)-1-((E)-4-((E)-2-((1-ethyl-3-methyl-1H-pyrazole-5-carbonyl)imino)-7-methoxy-5-(1-(2-(2-methoxyethoxy)ethyl)-1H-1,2,3-triazol-4-yl)-2,3-dihydro-1H-benzo[d]imidazol-1-yl)but-2-en-1-yl)-7-(3-morpholino-propoxy)-2,3-dihydro-1H-benzo[d]imidazole-5-carboxamide (**42**).* White solid; yield: 37%. HPLC purity: 96.8%. ^{1}H NMR (400 MHz, CD_3OD): δ 8.29 (d, J = 4.9 Hz, 1H), 7.49 (s, 1H), 7.42 (d, J = 4.4 Hz, 1H), 7.07 (d, J = 6.3 Hz, 1H), 7.01 (s, 1H), 6.59 (d, J = 4.7 Hz, 1H), 6.52 (d, J = 4.5 Hz, 1H), 5.72 (s, 2H), 4.90−4.78 (m, 4H), 4.58 (m, 6H), 3.97 (t, J = 5.0 Hz, 2H), 3.79 (s, 2H), 3.67 (m, 2H), 3.64−3.57 (m, 7H), 3.57−3.53 (m, 2H), 3.34 (s, 3H), 2.48 (br, 6H), 2.22−2.14 (m, 6H), 1.72 (s, 2H), 1.33 (m, 6H). ^{13}C NMR (151 MHz, CD_3OD): δ 169.36, 167.09, 151.68, 146.52, 145.75, 144.38, 139.91, 130.25, 129.46, 128.99, 127.70, 127.65, 126.40, 121.21, 117.11, 108.91, 108.83, 104.87, 103.74, 102.43, 100.95, 71.06, 69.37, 68.50, 66.36, 65.71, 57.29, 54.82, 54.33, 52.72, 49.71, 45.45, 44.02, 25.18, 14.85, 11.34, 11.32. MS (ESI, $[M + H]^+$) m/z, 976.4. HRMS (ESI) calcd for $C_{48}H_{62}N_{15}O_8^+$, 976.4900; found, 976.4874.

*(E)-1-((E)-4-((E)-5-Cyano-2-((1-ethyl-3-methyl-1H-pyrazole-5-carbonyl)imino)-7-(3-morpholinopropoxy)-2,3-dihydro-1H-benzo-[d]imidazol-1-yl)but-2-en-1-yl)-2-((1-ethyl-3-methyl-1H-pyrazole-5-carbonyl)imino)-7-methoxy-2,3-dihydro-1H-benzo[d]imidazole-5-carboxamide (**43**).* White solid; yield: 42%. HPLC purity: 98.0%. ^{1}H NMR (400 MHz, $CDCl_3$ + CD_3OD): δ 7.35 (s, 1H), 7.19 (s, 1H), 7.17 (d, J = 1.4 Hz, 1H), 6.80 (s, 1H), 6.49 (s, 1H), 6.44 (s, 1H), 5.72 (m, 2H), 4.86 (t, J = 4.5 Hz, 4H), 4.46 (q, J = 7.2 Hz, 4H), 3.84 (t, J = 6.5 Hz, 2H), 3.65 (s, 3H), 3.52 (br, 4H), 2.20 (br, 6H), 2.09 (s, 6H), 1.72−1.55 (m, 2H), 1.25 (m, 6H). ^{13}C NMR (151 MHz, CD_3OD): δ 169.43, 168.63, 168.39, 153.17, 152.96, 146.46, 146.36, 145.71, 145.33, 139.83, 129.90, 129.34, 128.60, 127.96, 121.27, 120.41, 118.63, 109.94, 109.70, 109.47, 109.03, 106.35, 105.50, 103.97, 67.45, 66.54, 55.65, 55.04, 53.32, 46.27, 45.05, 44.87, 25.64, 15.96, 15.93, 12.88, 12.82. MS (ESI, $[M + H]^+$) m/z, 832.4. HRMS (ESI) calcd for $C_{42}H_{50}N_{13}O_6^+$, 832.4002; found, 832.4003.

*(E)-2-((1-Ethyl-3-methyl-1H-pyrazole-5-carbonyl)imino)-1-((E)-4-((E)-2-((1-ethyl-3-methyl-1H-pyrazole-5-carbonyl)imino)-7-(3-morpholinopropoxy)-5-(1H-1,2,4-triazol-5-yl)-2,3-dihydro-1H-benzo-[d]imidazol-1-yl)but-2-en-1-yl)-7-methoxy-2,3-dihydro-1H-benzo-[d]imidazole-5-carboxamide (**44**).* White solid; yield: 36%. HPLC purity: 99.6%. ^{1}H NMR (400 MHz, CD_3OD): δ 8.39 (s, 1H), 7.63 (d, J = 1.1 Hz, 1H), 7.55 (d, J = 1.2 Hz, 1H), 7.27 (s, 1H), 7.20 (d, J = 1.3 Hz, 1H), 6.60 (s, 1H), 6.49 (s, 1H), 5.79 (qt, J = 15.5, 4.9 Hz, 2H), 4.93 (br, 4H), 4.60 (q, J = 7.1 Hz, 2H), 4.52 (q, J = 7.1 Hz, 2H),

https://dx.doi.org/10.1021/acs.jmedchem.0c01900
J. Med. Chem. 2021, 64, 1649−1669

3.86 (t, J = 6.1 Hz, 2H), 3.68 (s, 3H), 3.60 (t, J = 4.6 Hz, 4H), 2.43−2.26 (m, 6H), 2.21 (s, 3H), 2.13 (s, 3H), 1.69 (m, 2H), 1.36 (t, J = 7.1 Hz, 4H), 1.30 (t, J = 7.1 Hz, 4H). ^{13}C NMR (126 MHz, CD_3OD): δ 171.20, 169.06, 154.04, 147.65, 147.58, 147.01, 146.79, 141.50, 131.56, 130.92, 129.97, 129.12, 121.79, 110.70, 106.26, 105.92, 105.58, 68.22, 67.65, 56.66, 56.38, 54.63, 49.00, 47.29, 45.94, 27.07, 16.67, 16.62, 13.17, 13.14. MS (ESI, $[M + H]^+$) m/z, 874.4. HRMS (ESI) calcd for $C_{43}H_{52}N_{15}O_6^+$, 874.4220; found, 874.4227.

*(E)-2-((1-Ethyl-3-methyl-1H-pyrazole-5-carbonyl)imino)-1-((E)-4-((E)-2-((1-ethyl-3-methyl-1H-pyrazole-5-carbonyl)imino)-5-(1H-imidazol-2-yl)-7-(3-morpholinopropoxy)-2,3-dihydro-1H-benzo[d]-imidazol-1-yl)but-2-en-1-yl)-7-methoxy-2,3-dihydro-1H-benzo[d]-imidazole-5-carboxamide (**45**).* White solid; yield: 31%. HPLC purity: 95.2%. ^{1}H NMR (400 MHz, CD_3OD): δ 7.51 (d, J = 1.4 Hz, 1H), 7.40 (d, J = 1.3 Hz, 1H), 7.16 (d, J = 1.5 Hz, 1H), 7.13 (s, 2H), 7.09 (d, J = 1.4 Hz, 1H), 6.56 (s, 1H), 6.46 (s, 1H), 5.83−5.68 (m, 2H), 4.89 (br, 4H), 4.57 (q, J = 7.1 Hz, 2H), 4.48 (q, J = 7.1 Hz, 2H), 3.80 (t, J = 6.1 Hz, 2H), 3.62 (s, 3H), 3.60−3.53 (m, 4H), 2.35−2.21 (m, 6H), 2.18 (s, 3H), 2.10 (s, 3H), 1.65 (m, 2H), 1.33 (t, J = 7.1 Hz, 3H), 1.27 (t, J = 7.1 Hz, 3H). ^{13}C NMR (126 MHz, CD_3OD): δ 171.22, 169.01, 153.98, 147.69, 147.60, 147.55, 146.95, 146.81, 141.48, 131.49, 130.88, 129.93, 129.14, 127.75, 121.72, 110.72, 110.66, 106.21, 105.84, 104.77, 68.16, 67.61, 56.67, 56.32, 54.61, 49.51, 49.34, 49.17, 49.00, 48.83, 48.66, 48.49, 48.49, 47.29, 47.25, 45.91, 45.87, 27.07, 16.67, 16.63, 13.17, 13.13. MS (ESI, $[M + H]^+$) m/z, 873.4. HRMS (ESI) calcd for $C_{44}H_{53}N_{14}O_6^+$, 873.4267; found, 873.4264.

*(E)-2-((1-Ethyl-3-methyl-1H-pyrazole-5-carbonyl)imino)-1-((E)-4-((E)-2-((1-ethyl-3-methyl-1H-pyrazole-5-carbonyl)imino)-7-methoxy-5-(1H-1,2,4-triazol-5-yl)-2,3-dihydro-1H-benzo[d]imidazol-1-yl)but-2-en-1-yl)-7-(3-hydroxypropoxy)-2,3-dihydro-1H-benzo[d]-imidazole-5-carboxamide (**48**).* White solid; yield: 38%. HPLC purity: 99.5%. ^{1}H NMR (600 MHz, DMSO): δ 12.81 (br, 2H), 8.47 (s, 2H), 7.96 (s, 1H), 7.81 (s, 1H), 7.63 (s, 1H), 7.44 (d, J = 1.2 Hz, 1H), 7.31 (s, 1H), 6.50 (d, J = 3.2 Hz, 2H), 5.94−5.75 (m, 2H), 4.92 (d, J = 4.1 Hz, 2H), 4.90 (d, J = 4.3 Hz, 2H), 4.57−4.46 (m, 4H), 4.06 (t, J = 6.4 Hz, 2H), 3.75 (s, 3H), 3.43 (t, J = 6.0 Hz, 2H), 2.09 (s, 3H), 2.07 (s, 3H), 1.71 (p, 2H), 1.25 (m, 6H). ^{13}C NMR (151 MHz, DMSO): δ 167.50, 167.45, 166.77, 151.98, 151.62, 145.50, 145.01, 144.28, 139.90, 130.62, 129.95, 128.18, 127.96, 119.59, 109.20, 105.43, 105.21, 103.48, 103.12, 65.90, 57.09, 55.79, 45.56, 44.59, 31.81, 16.12, 13.10, 13.08. MS (ESI, $[M + H]^+$) m/z, 805.4. HRMS (ESI) calcd for $C_{39}H_{45}N_{14}O_6^+$, 805.3641; found, 805.3636.

Compounds **55** and **56** were prepared by following similar procedures as described above.

*(E)-2-((1-Ethyl-3-methyl-1H-pyrazole-5-carbonyl)imino)-1-((E)-4-((E)-2-((1-ethyl-3-methyl-1H-pyrazole-5-carbonyl)imino)-7-methoxy-5-(1H-1,2,4-triazol-5-yl)-2,3-dihydro-1H-benzo[d]imidazol-1-yl)but-2-en-1-yl)-2,3,7,8-tetrahydro-1H-[1,4]dioxino[2′,3′:3,4]-benzo[1,2-d]imidazole-5-carboxamide (**55**).* White solid. HPLC purity: 99.2%. ^{1}H NMR (400 MHz, DMSO): δ 12.82 (br, 1H), 12.66 (s, 1H), 8.60 (br, 1H), 7.82 (s, 1H), 7.54 (s, 1H), 7.52 (s, 1H), 7.46 (s, 1H), 6.53 (s, 1H), 6.51 (s, 1H), 5.85 (s, 2H), 4.92 (s, 2H), 4.85 (s, 2H), 4.59−4.42 (m, 4H), 4.29 (s, 2H), 4.19 (s, 2H), 3.80 (s, 3H), 2.10 (s, 3H), 2.07 (s, 3H), 1.34−1.23 (m, 6H). ^{13}C NMR (126 MHz, DMSO): δ 166.78, 165.47, 152.18, 151.69, 145.52, 145.01, 139.82, 138.26, 130.69, 129.54, 128.25, 127.94, 123.39, 119.69, 118.52, 109.20, 106.04, 103.52, 103.15, 64.22, 63.82, 55.79, 45.54, 44.68, 44.42, 16.11, 16.07, 13.06, 13.04. MS (ESI, $[M - H]^-$) m/z, 787.3. HRMS (ESI) calcd for $C_{38}H_{39}N_{14}O_6^-$, 787.3182; found, 787.3165.

*(E)-2-((1-Ethyl-3-methyl-1H-pyrazole-5-carbonyl)imino)-1-((E)-4-((E)-2-((1-ethyl-3-methyl-1H-pyrazole-5-carbonyl)imino)-7-methoxy-5-(1H-1,2,4-triazol-5-yl)-2,3-dihydro-1H-benzo[d]imidazol-1-yl)but-2-en-1-yl)-2,3-dihydro-1H-benzofuro[6,7-d]imidazole-5-carboxamide (**56**).* White solid. HPLC purity: 100%. ^{1}H NMR (600 MHz, $CDCl_3$ + CD_3OD): δ 8.14 (br, 1H), 7.59 (s, 1H), 7.49 (br, 1H), 7.29 (d, J = 2.1 Hz, 1H), 7.17 (d, J = 2.1 Hz, 1H), 7.15 (s, 1H), 6.62 (s, 1H), 6.54 (s, 1H), 6.01 (m, 1H), 5.87 (m, 1H), 5.01 (d, J = 6.3 Hz, 2H), 4.94 (d, J = 6.0 Hz, 2H), 4.59 (m, 2H), 4.54 (q, J = 7.1 Hz, 2H), 3.50 (s, 3H), 2.19 (s, 3H), 2.18 (s, 3H), 1.39 (t, J = 7.2 Hz, 3H), 1.36 (t, J = 7.1 Hz, 3H). ^{13}C NMR (151 MHz, DMSO): δ 168.38, 166.78, 151.68, 145.81, 145.50, 145.14, 145.05, 139.95, 138.79, 130.69, 128.61, 126.82, 126.20, 123.18, 122.62, 118.26, 116.37, 109.22, 108.03, 103.52, 103.16, 55.73, 45.66, 45.61, 44.64, 16.14, 16.11, 13.13, 13.11. MS (ESI, $[M + H]^+$) m/z, 771.4. HRMS (ESI) calcd for $C_{38}H_{39}N_{14}O_5^+$, 771.3222; found, 771.3214.

Conversion of **57** and **27c** to target compounds **64**−**66** were conducted by following a similar procedure as described above.

*(E)-2-((1-Ethyl-3-methyl-1H-pyrazole-5-carbonyl)imino)-1-(4-((E)-2-((1-ethyl-3-methyl-1H-pyrazole-5-carbonyl)imino)-7-methoxy-5-(1H-1,2,4-triazol-5-yl)-2,3-dihydro-1H-benzo[d]imidazol-1-yl)butyl)-7-(3-morpholinopropoxy)-2,3-dihydro-1H-benzo[d]-imidazole-5-carboxamide (**64**).* White solid. HPLC purity: 100%. ^{1}H NMR (500 MHz, DMSO): δ 12.77 (s, 2H), 7.96 (s, 1H), 7.78 (s, 1H), 7.57 (s, 1H), 7.47 (s, 1H), 7.30 (s, 2H), 6.58 (s, 1H), 6.54 (s, 1H), 4.56 (m, 4H), 4.36 (s, 4H), 4.09 (t, J = 6.2 Hz,2H), 3.88 (s, 3H), 3.41 (t, J = 4.6 Hz, 4H), 2.30 (t, J = 7.1 Hz, 2H), 2.18 (br, 4H), 2.09 (s, 3H), 2.08 (s, 3H), 1.86 (br, 4H), 1.83−1.73 (m, 2H), 1.30 (m, 6H). ^{13}C NMR (126 MHz, DMSO): δ 167.68, 166.84, 152.24, 145.38, 144.98, 144.08, 140.01, 130.00, 119.65, 109.16, 105.45, 105.21, 103.32, 66.88, 66.02, 55.90, 54.85, 53.20, 45.57, 43.32, 26.67, 25.78, 16.15, 13.11. MS (ESI, $[M + H]^+$) m/z, 876.5. HRMS (ESI) calcd for $C_{43}H_{54}N_{15}O_6^+$, 876.4376; found, 876.4376.

*(E)-2-((1-Ethyl-3-methyl-1H-pyrazole-5-carbonyl)imino)-1-((1s,4s)-4-((E)-2-((1-ethyl-3-methyl-1H-pyrazole-5-carbonyl)imino)-7-methoxy-5-(1H-1,2,4-triazol-5-yl)-2,3-dihydro-1H-benzo[d]-imidazol-1-yl)cyclohexyl)-7-(3-morpholinopropoxy)-2,3-dihydro-1H-benzo[d]imidazole-5-carboxamide (**65**).* White solid. HPLC purity: 99.6% (H_2O/MeOH and 0.1% DEA); 99.4% (H_2O/MeCN and 0.1% DEA). ^{1}H NMR (400 MHz, DMSO): δ 14.16 (s, 1H), 13.00 (s, 2H), 8.63 (s, 1H), 8.06 (s, 1H), 7.93 (s, 1H), 7.72 (s, 1H), 7.60 (s, 1H), 7.44 (s, 1H), 7.41 (s, 1H), 6.70 (s, 1H), 6.66 (s, 1H), 5.61 (br, 2H), 5.51 (br, 1H), 4.63 (s, 4H), 4.34 (s, 2H), 4.02 (s, 3H), 3.44 (s, 4H), 2.92 (br, 4H), 2.45 (s, 2H), 2.30 (s, 4H), 2.19−1.88 (m, 12H), 1.38 (t, J = 7.2 Hz, 6H). MS (ESI, $[M + H]^+$) m/z, 902.4. HRMS (ESI) calcd for $C_{45}H_{56}N_{15}O_6^+$, 902.4533; found, 902.4517.

*(E)-2-((1-Ethyl-3-methyl-1H-pyrazole-5-carbonyl)imino)-1-((1r,4r)-4-((E)-2-((1-ethyl-3-methyl-1H-pyrazole-5-carbonyl)imino)-7-methoxy-5-(1H-1,2,4-triazol-5-yl)-2,3-dihydro-1H-benzo[d]-imidazol-1-yl)cyclohexyl)-7-(3-morpholinopropoxy)-2,3-dihydro-1H-benzo[d]imidazole-5-carboxamide (**66**).* White solid. HPLC purity: 95.5% (H_2O/MeOH and 0.1% DEA); 95.0% (H_2O/MeCN and 0.1% DEA). ^{1}H NMR (400 MHz, $CDCl_3$ + CD_3OD): δ 8.19 (s, 1H), 7.64 (s, 1H), 7.59 (s, 1H), 7.47 (s, 2H), 6.74 (s, 1H), 6.68 (s, 1H), 5.36 (s, 2H), 4.65 (m, 4H), 4.50−4.09 (m, 5H), 3.64 (s, 4H), 3.08 (br, 1H), 2.65 (br, 2H), 2.40 (br, 4H), 2.26 (s, 6H), 2.20−1.90 (m, 8H), 1.52−1.40 (m, 6H). MS (ESI, $[M + H]^+$) m/z, 902.4. HRMS (ESI) calcd for $C_{45}H_{56}N_{15}O_6^+$, 902.4533; found, 902.4532.

General Procedure for Synthesis of HCl Salt of 5 and 40. To a solution of compound **5** or **40** (0.1 mmol) in MeOH (10 mL) was added 4 N HCl in 1,4-dioxane (1 mL). The mixture was stirred at room temperature for 4 h and concentrated in vacuo. After repeating the above operation twice, a white-like solid was formed, washed with EtOH, and dried under an infrared-ray oven. HCl salt of **5** or **40** was obtained. For **40**·3HCl·2.5H_2O ($C_{43}H_{51}N_{15}O_6$·3HCl·2.5H_2O), calcd: C, 50.22; H, 5.78; N, 20.43; found: C, 50.30; H, 5.83; N, 20.23; For **5**·3H_2O·H_2O ($C_{42}H_{56}Cl_3N_{13}O_8$·3HCl·$H_2O$), calcd: C, 51.61; H, 5.78; N, 18.63; found: C, 51.63; H, 5.98; N, 18.57.

Reagents. DMXAA (cat. code: MB3940) was purchased from Meilunbio (Liaoning, China), and ADU-S100 (cat. code: tlrl-nacda2r), QUANTI-Luc solution (cat. code: rep-qlc2), and QUANTI-Blue solution (cat. code: rep-qlc2) were purchased from InvivoGen (San Diego, USA). Antibodies against phospho-TBK1 (Ser172) (cat. code: 5483S), TBK1 (cat. code: 3504S), phospho-IRF3 (Ser396) (cat. code:4947S), IRF3 (cat. code: 4302S), and GAPDH (cat. code: 5174S) were purchased from Cell Signaling Technology (Beverly, MA). Cytosolic fragments (139−379) of human STING protein (R232, H232, 293Q, and AQ) and mouse STING (R231) were purchased from Novoprotein (Shanghai, China).

Cell lines THP1-Blue-ISG cells (cat. code: thp-isg), THP-1-Dual cells (cat.code:thpd-nfis), THP1-Dual-KO-STING cells (cat. code:

https://dx.doi.org/10.1021/acs.jmedchem.0c01900
J. Med. Chem. 2021, 64, 1649−1669

thpd-kostg), 293T-Dual hSTING-H232 cells (cat. code: 293d-h232), 293T-Dual hSTING-R232 cells (cat. code: 293d-r232), RAW-Lucia (cat. code: rawl-isg), and RAW-Lucia-KO-STING (cat. code: rawl-kostg) were purchased from InvivoGen (San Diego, USA). Zeocin (cat. code: ant-zn-05), Normocin (cat. code: ant-nr-1), and blastcidin (cat. code: ant-bl-1) were purchased from InvivoGen (San Diego, USA). All the cells were cultured according to the manufacture's protocol and incubated at 37 °C in a humidified atmosphere of 5% CO_2 and 95% air.

ISG-Reporter Assay. THP1-Blue-ISG cells or other reporter cells as indicated (1×10^5 cells/well) were suspended in 180 μL of medium and added to 96-well plates, and then indicated concentrations of compound (20 μL) were added to the cells for 24 h. Subsequently, 20 μL of supernatant and 50 μL of QUANTI-Luc detection reagent (or 180 μL of QUNTI-Blue SEAP detection reagent for THP1-Blue-ISG) were added into a 96-well black plate (cat. code: 3601; Corning). The luminescence and absorbance at 650 nm were measured by SpectraMAX Paradigm and SpectraMAX Plus 384 (Molecular Devices, Sunnyvale, CA), respectively.

NF-kB Reporter Assay. THP1-Dual cells (1×10^5 cells/well) were suspended in 180 μL of medium and added to 96-well plates, and indicated concentrations of compound (20 μL) were then added to the cells for 24 h. Subsequently, 20 μL of supernatant and 180 μL of QUANTI-Blue detection reagent were incubated at 37 °C in a humidified atmosphere of 5% CO_2 and 95% air. After 1 h, the absorbance was measured at 650 nm by a SpectraMAX Plus 384 (Molecular Devices, Sunnyvale, CA).

Enzyme-Linked Immunosorbent Assay. THP1-Dual cells were seeded in 96-well plates at a density of 10^5 cells/well and treated with indicated concentrations of **5** or **40** for 24 h. Cell supernatants were used to test the level of cytokines. Human IP-10 and IFN-β levels in the supernatant were determined using a human IP-10 ELISA kit (cat. code: 550926; BD) and human interferon-beta (IFN-β) kit (cat. code: AL265C; PerkinElmer, MA, USA) according to the protocol. The cytokine concentration (pg/mL) was calculated according to the standard curve, and histograms were made by GraphPad Prism 8. The test was carried out in triplicates.

Western Blotting. THP1-Dual cells (8×10^5 cells/well) were seeded into 6-well plate and treated with compound **5** or **40** (3.3, 10, and 30 μM) for 4 h. Cell lysates were harvested using 1× SDS-PAGE sample loading buffer (cat. code: P0015; Beyotime, China) and boiled at 100 °C for 30 min. Cell lysates were run on 10% SDS-PAGE gels and transferred onto NC membranes. The membranes were probed with anti-TBK1, phospho-TBK1 (Ser172), anti-IRF3, anti-phospho-IRF3 (Ser396), and anti-GAPDH. Horseradish peroxidase-conjugated secondary antibodies were used as secondary antibodies. Finally, the membrane was detected by enhanced chemiluminescence (ECL Plus; cat. code: 17050622; Bio-Rad).

Differential Scanning Fluorimetry Assay. Differential scanning fluorimetry (DSF) was used to evaluate the binding of compound to STING protein. SYPRO Orange dye (10×) (cat.code: S6651; Life Technologies), STING protein (5 μM), and compound (50 μM) were mixed in the 40 μL of reaction buffer, which contained 10 mM HEPES (pH 7.5) and 150 mM NaCl. Then, the reaction mixture was transferred to a 96-well plate and measured by a CFX96 real-time system (Bio-Rad, CA, USA). Briefly, the fluorescence intensity was monitored as the run program, and the initial temperature was at 30 °C followed by a temperature gradient in which the samples are heated at a scan rate of 0.5 °C/min until a final temperature of 80 °C. T_m was calculated as the temperature of median fluorescence from the initial increase to the highest fluorescence intensity.

Animal Studies. Animal procedures were approved by the Institutional Animal Care and Use Committee of the Shanghai Institute of Materia Medica. BALB/c female mice (6 weeks) were purchased from LingChang Biotechnology (Shanghai, China). 4T1 cells (5×10^5) were inoculated into the breast fat pad of each mice. CT26 cells (5×10^5) were injected subcutaneously into the right armpit of each mice. When the tumors grew to approximately 50−100 mm^3, the mice were treated with the indicated compound. The 4T1 tumor model ($n = 5$) was treated with compound **40** (10 mg/kg) or **5** (10 mg/kg) on days 1, 4, and 7. The CT26 tumor model ($n = 6$) was treated with **40** (500 μg/IT) or DMXAA (250 μg/IT) on days 1, 4, and 7. Tumor volume and body weight were measured twice per week. Tumor volume (TV) was calculated by the formula: $V = (a \times b^2)/2$ (a, width; b, length).

■ ASSOCIATED CONTENT

Supporting Information

The Supporting Information is available free of charge at https://pubs.acs.org/doi/10.1021/acs.jmedchem.0c01900.

Docking mode of compound **40** with h-STING, ^1H and ^{13}C spectra of all new compounds, preparation and elemental analysis of HCl salt of **5** and **40**, and aqueous solubility of HCl salts of **5** and **40** (PDF)

Molecular formula strings and some data (CSV)

■ AUTHOR INFORMATION

Corresponding Authors

Zuoquan Xie − *State Key Laboratory of Drug Research, Shanghai Institute of Materia Medica (SIMM), Chinese Academy of Sciences, Shanghai 201203, China; University of Chinese Academy of Sciences, Beijing 100049, China*; Phone: +86-21-50806072; Email: zqxie@simm.ac.cn

Ao Zhang − *State Key Laboratory of Drug Research, Shanghai Institute of Materia Medica (SIMM), Chinese Academy of Sciences, Shanghai 201203, China; Shanghai Key Laboratory for Molecular Engineering of Chiral Drugs, School of Pharmacy, Shanghai Jiao Tong University, Shanghai 200240, China; College of Pharmacy, Nanjing University of Chinese Medicine, Nanjing 210023, China; University of Chinese Academy of Sciences, Beijing 100049, China; State Key Laboratory of Esophageal Cancer Prevention and Treatment, Ministry of Education of China, Zhengzhou University, Zhengzhou 450001, China*; orcid.org/0000-0001-7205-9202; Phone: +86-21-34204020; Email: ao6919zhang@sjtu.edu.cn

Authors

Zilan Song − *State Key Laboratory of Drug Research, Shanghai Institute of Materia Medica (SIMM), Chinese Academy of Sciences, Shanghai 201203, China; Shanghai Key Laboratory for Molecular Engineering of Chiral Drugs, School of Pharmacy, Shanghai Jiao Tong University, Shanghai 200240, China; College of Pharmacy, Nanjing University of Chinese Medicine, Nanjing 210023, China*

Xiyuan Wang − *State Key Laboratory of Drug Research, Shanghai Institute of Materia Medica (SIMM), Chinese Academy of Sciences, Shanghai 201203, China; University of Chinese Academy of Sciences, Beijing 100049, China*

Yan Zhang − *State Key Laboratory of Drug Research, Shanghai Institute of Materia Medica (SIMM), Chinese Academy of Sciences, Shanghai 201203, China; University of Chinese Academy of Sciences, Beijing 100049, China*

Wangting Gu − *State Key Laboratory of Drug Research, Shanghai Institute of Materia Medica (SIMM), Chinese Academy of Sciences, Shanghai 201203, China; Shanghai Key Laboratory for Molecular Engineering of Chiral Drugs, School of Pharmacy, Shanghai Jiao Tong University, Shanghai 200240, China*

Ancheng Shen − *State Key Laboratory of Drug Research, Shanghai Institute of Materia Medica (SIMM), Chinese Academy of Sciences, Shanghai 201203, China; Shanghai Key Laboratory for Molecular Engineering of Chiral Drugs,*

School of Pharmacy, Shanghai Jiao Tong University, Shanghai 200240, China

Chunyong Ding − *Shanghai Key Laboratory for Molecular Engineering of Chiral Drugs, School of Pharmacy, Shanghai Jiao Tong University, Shanghai 200240, China*

Han Li − *State Key Laboratory of Drug Research, Shanghai Institute of Materia Medica (SIMM), Chinese Academy of Sciences, Shanghai 201203, China; College of Pharmacy, Nanjing University of Chinese Medicine, Nanjing 210023, China*

Ruoxuan Xiao − *Shanghai Key Laboratory for Molecular Engineering of Chiral Drugs, School of Pharmacy, Shanghai Jiao Tong University, Shanghai 200240, China*

Meiyu Geng − *State Key Laboratory of Drug Research, Shanghai Institute of Materia Medica (SIMM), Chinese Academy of Sciences, Shanghai 201203, China; University of Chinese Academy of Sciences, Beijing 100049, China*

Complete contact information is available at: https://pubs.acs.org/10.1021/acs.jmedchem.0c01900

Author Contributions

[#]Z.S., X.W., and Y.Z. contributed equally to this work.

Notes

The authors declare no competing financial interest.

■ ACKNOWLEDGMENTS

This work was supported by grants from Chinese NSF (grants 81703327 and 81773565) and "Personalized Medicines-Molecular Signature-based Drug Discovery and Development", Strategic Priority Research Program of the Chinese Academy of Sciences (grant nos. XDA12020366 and XDA12020226). Supporting grants from the National Science & Technology Major Project "Key New Drug Creation and Manufacturing Program" (grant nos. 2018ZX09711002-11-021 and 2018ZX09711002-017) as well as a start-up grant to the Research Laboratory of Medicinal Chemical Biology & Frontiers on Drug Discovery (AF1700037 and WF220217002) from Shanghai Jiao Tong University and Shanghai Pujiang Program (18PJD052) are also appreciated.

■ ABBREVIATIONS USED

STING, stimulator of interferon gene; CDN, cyclic dinucleotide; mAbs, monoclonal antibodies; IO, immuno-oncology; GMP, guanosine monophosphate; AMP, adenosine monophosphate; cGAS, cyclic GMP-AMP synthase; IFN, interferon; IT, intratumoral; DMXAA, 5,6-dimethylxanthenone-4-acetic acid; CMA, 10-carboxymethyl-9-acridanone; ABZI, amidobenzimidazole; SAR, structure−activity relationship; PK, pharmacokinetic; SEAP, secreted embryonic alkaline phosphatase; ISG, interferon-stimulated gene; DSF, differential scanning fluorimetry; ECL, enhanced chemiluminescence; V_{ss}, volume of distribution; $T_{1/2}$, half-life; C_{max}, maximum concentration; $AUC_{0-\infty}$, area under the plasma concentration time curve

■ REFERENCES

(1) Chen, L.; Flies, D. B. Molecular mechanisms of T cell co-stimulation and co-inhibition. *Nat. Rev. Immunol.* **2013**, *13*, 227−242.

(2) Darvin, P.; Toor, S. M.; Nair, V. S.; Elkord, E. Immune checkpoint inhibitors: recent progress and potential biomarkers. *Exp. Mol. Med.* **2018**, *50*, 1−11.

(3) Marhelava, K.; Pilch, Z.; Bajor, M.; Graczyk-Jarzynka, A.; Zagozdzon, R. Targeting negative and positive immune checkpoints with monoclonal antibodies in therapy of cancer. *Cancers* **2019**, *11*, 1756.

(4) Adams, J. L.; Smothers, J.; Srinivasan, R.; Hoos, A. Big opportunities for small molecules in immuno-oncology. *Nat. Rev. Drug Discovery* **2015**, *14*, 603−622.

(5) Huck, B. R.; Kötzner, L.; Urbahns, K. Small molecules drive big improvements in immuno-oncology therapies. *Angew. Chem., Int. Ed.* **2018**, *57*, 4412−4428.

(6) Chen, S.; Song, Z.; Zhang, A. Small-molecule immuno-oncology therapy: advances, challenges and new directions. *Curr. Top. Med. Chem.* **2019**, *19*, 180−185.

(7) Ishikawa, H.; Barber, G. N. STING is an endoplasmic reticulum adaptor that facilitates innate immune signalling. *Nature* **2008**, *455*, 674−678.

(8) Ishikawa, H.; Ma, Z.; Barber, G. N. STING regulates intracellular DNA-mediated, type I interferon-dependent innate immunity. *Nature* **2009**, *461*, 788−792.

(9) Chen, Q.; Sun, L.; Chen, Z. J. Regulation and function of the cGAS-STING pathway of cytosolic DNA sensing. *Nat. Immunol.* **2016**, *17*, 1142−1149.

(10) Sun, L.; Wu, J.; Du, F.; Chen, X.; Chen, Z. J. Cyclic GMP-AMP synthase is a cytosolic DNA sensor that activates the type I interferon pathway. *Science* **2013**, *339*, 786−791.

(11) Zhang, C.; Shang, G.; Gui, X.; Zhang, X.; Bai, X.-c.; Chen, Z. J. Structural basis of STING binding with and phosphorylation by TBK1. *Nature* **2019**, *567*, 394−398.

(12) Tanaka, Y.; Chen, Z. J. STING specifies IRF3 phosphorylation by TBK1 in the cytosolic DNA signaling pathway. *Sci. Signaling* **2012**, *5*, ra20.

(13) Liu, S.; Cai, X.; Wu, J.; Cong, Q.; Chen, X.; Li, T.; Du, F.; Ren, J.; Wu, Y.-T.; Grishin, N. V.; Chen, Z. J. Phosphorylation of innate immune adaptor proteins MAVS, STING, and TRIF induces IRF3 activation. *Science* **2015**, *347*, No. aaa2630.

(14) Barber, G. N. STING: infection, inflammation and cancer. *Nat. Rev. Immunol.* **2015**, *15*, 760−770.

(15) Zhang, H.; You, Q.-D.; Xu, X.-L. Targeting stimulator of interferon genes (STING): a medicinal chemistry perspective. *J. Med. Chem.* **2020**, *63*, 3785−3816.

(16) Ding, C.; Song, Z.; Shen, A.; Chen, T.; Zhang, A. Small molecules targeting the innate immune cGAS−STING−TBK1 signaling pathway. *Acta Pharm. Sin. B* **2020**, *10*, 2272−2298.

(17) Fu, J.; Kanne, D. B.; Leong, M.; Glickman, L. H.; McWhirter, S. M.; Lemmens, E.; Mechette, K.; Leong, J. J.; Lauer, P.; Liu, W.; Sivick, K. E.; Zeng, Q.; Soares, K. C.; Zheng, L.; Portnoy, D. A.; Woodward, J. J.; Pardoll, D. M.; Dubensky, T. W., Jr.; Kim, Y. STING agonist formulated cancer vaccines can cure established tumors resistant to PD-1 blockade. *Sci. Transl. Med.* **2015**, *7*, 283ra52.

(18) Corrales, L.; Glickman, L. H.; McWhirter, S. M.; Kanne, D. B.; Sivick, K. E.; Katibah, G. E.; Woo, S.-R.; Lemmens, E.; Banda, T.; Leong, J. J.; Metchette, K.; Dubensky, T. W., Jr.; Gajewski, T. F. Direct activation of STING in the tumor microenvironment leads to potent and systemic tumor regression and immunity. *Cell Rep.* **2015**, *11*, 1018−1030.

(19) Corrales, L.; McWhirter, S. M.; Dubensky, T. W., Jr.; Gajewski, T. F. The host STING pathway at the interface of cancer and immunity. *J. Clin. Invest.* **2016**, *126*, 2404−2411.

(20) Meric-Bernstam, F.; Sandhu, S. K.; Hamid, O.; Spreafico, A.; Kasper, S.; Dummer, R.; Shimizu, T.; Steeghs, N.; Lewis, N.; Talluto, C. C.; Dolan, S.; Bean, A.; Brown, R.; Trujillo, D.; Nair, N.; Luke, J. J. Phase Ib study of MIW815 (ADU-S100) in combination with spartalizumab (PDR001) in patients (pts) with advanced/metastatic solid tumors or lymphomas. *J. Clin. Oncol.* **2019**, *37*, 2507−2507.

(21) Conlon, J.; Burdette, D. L.; Sharma, S.; Bhat, N.; Thompson, M.; Jiang, Z.; Rathinam, V. A. K.; Monks, B.; Jin, T.; Xiao, T. S.; Vogel, S. N.; Vance, R. E.; Fitzgerald, K. A. Mouse, but not human STING, binds and signals in response to the vascular disrupting agent 5,6-dimethylxanthenone-4-acetic acid. *J. Immunol.* **2013**, *190*, 5216−5225.

(22) Gao, P.; Zillinger, T.; Wang, W.; Ascano, M.; Dai, P.; Hartmann, G.; Tuschl, T.; Deng, L.; Barchet, W.; Patel, D. J. Binding-pocket and lid-region substitutions render human STING sensitive to the species-specific drug DMXAA. *Cell Rep.* **2014**, *8*, 1668−1676.
(23) Cavlar, T.; Deimling, T.; Ablasser, A.; Hopfner, K. P.; Hornung, V. Species-specific detection of the antiviral small-molecule compound CMA by STING. *EMBO J.* **2013**, *32*, 1440−1450.
(24) Ramanjulu, J. M.; Pesiridis, G. S.; Yang, J.; Concha, N.; Singhaus, R.; Zhang, S.-Y.; Tran, J.-L.; Moore, P.; Lehmann, S.; Eberl, H. C.; Muelbaier, M.; Schneck, J. L.; Clemens, J.; Adam, M.; Mehlmann, J.; Romano, J.; Morales, A.; Kang, J.; Leister, L.; Graybill, T. L.; Charnley, A. K.; Ye, G.; Nevins, N.; Behnia, K.; Wolf, A. I.; Kasparcova, V.; Nurse, K.; Wang, L.; Puhl, A. C.; Li, Y.; Klein, M.; Hopson, C. B.; Guss, J.; Bantscheff, M.; Bergamini, G.; Reilly, M. A.; Lian, Y.; Duffy, K. J.; Adams, J.; Foley, K. P.; Gough, P. J.; Marquis, R. W.; Smothers, J.; Hoos, A.; Bertin, J. Design of amidobenzimidazole STING receptor agonists with systemic activity. *Nature* **2018**, *564*, 439−443.
(25) Xi, Q.; Wang, M.; Jia, W.; Yang, M.; Hu, J.; Jin, J.; Chen, X.; Yin, D.; Wang, X. Design, synthesis, and biological evaluation of amidobenzimidazole derivatives as stimulator of interferon genes (STING) receptor agonists. *J. Med. Chem.* **2020**, *63*, 260−282.
(26) Pan, B.-S.; Perera, S. A.; Piesvaux, J. A.; Presland, J. P.; Schroeder, G. K.; Cumming, J. N.; Trotter, B. W.; Altman, M. D.; Buevich, A. V.; Cash, B.; Cemerski, S.; Chang, W.; Chen, Y.; Dandliker, P. J.; Feng, G.; Haidle, A.; Henderson, T.; Jewell, J.; Kariv, I.; Knemeyer, I.; Kopinja, J.; Lacey, B. M.; Laskey, J.; Lesburg, C. A.; Liang, R.; Long, B. J.; Lu, M.; Ma, Y.; Minnihan, E. C.; O'Donnell, G.; Otte, R.; Price, L.; Rakhilina, L.; Sauvagnat, B.; Sharma, S.; Tyagarajan, S.; Woo, H.; Wyss, D. F.; Xu, S.; Bennett, D. J.; Addona, G. H. An orally available non-nucleotide STING agonist with antitumor activity. *Science* **2020**, *369*, No. eaba6098.
(27) Chin, E. N.; Yu, C.; Vartabedian, V. F.; Jia, Y.; Kumar, M.; Gamo, A. M.; Vernier, W.; Ali, S. H.; Kissai, M.; Lazar, D. C.; Nguyen, N.; Pereira, L. E.; Benish, B.; Woods, A. K.; Joseph, S. B.; Chu, A.; Johnson, K. A.; Sander, P. N.; Martínez-Peña, F.; Hampton, E. N.; Young, T. S.; Wolan, D. W.; Chatterjee, A. K.; Schultz, P. G.; Petrassi, H. M.; Teijaro, J. R.; Lairson, L. L. Antitumor activity of a systemic STING-activating non-nucleotide cGAMP mimetic. *Science* **2020**, *369*, 993−999.
(28) Charnley, A. K.; Darcy, M. G.; Dodson, J. W.; Dong, X.; Hughes, T. V.; Kang, J.; Leister, L. K.; Lian, Y.; Li, Y.; Mehlmann, J.; Nevins, N.; Ramanjulu, J. M.; Romano, J. J.; Wang, G. Z.; Ye, G.; Zhang, D. Heterocyclic amides useful as protein modulators. WO2017175147A1, Oct 12, 2017, DOI: 10.18632/oncotarget.19106.
(29) Patel, S.; Jin, L. *TMEM173* variants and potential importance to human biology and disease. *Genes. Immun.* **2019**, *20*, 82−89.

https://dx.doi.org/10.1021/acs.jmedchem.0c01900
J. Med. Chem. 2021, 64, 1649−1669